Leonid Andreev, Dmitry Andreev. FIG. 1 of 43. A flow diagram of MeaningFinder™ algorithmic architecture

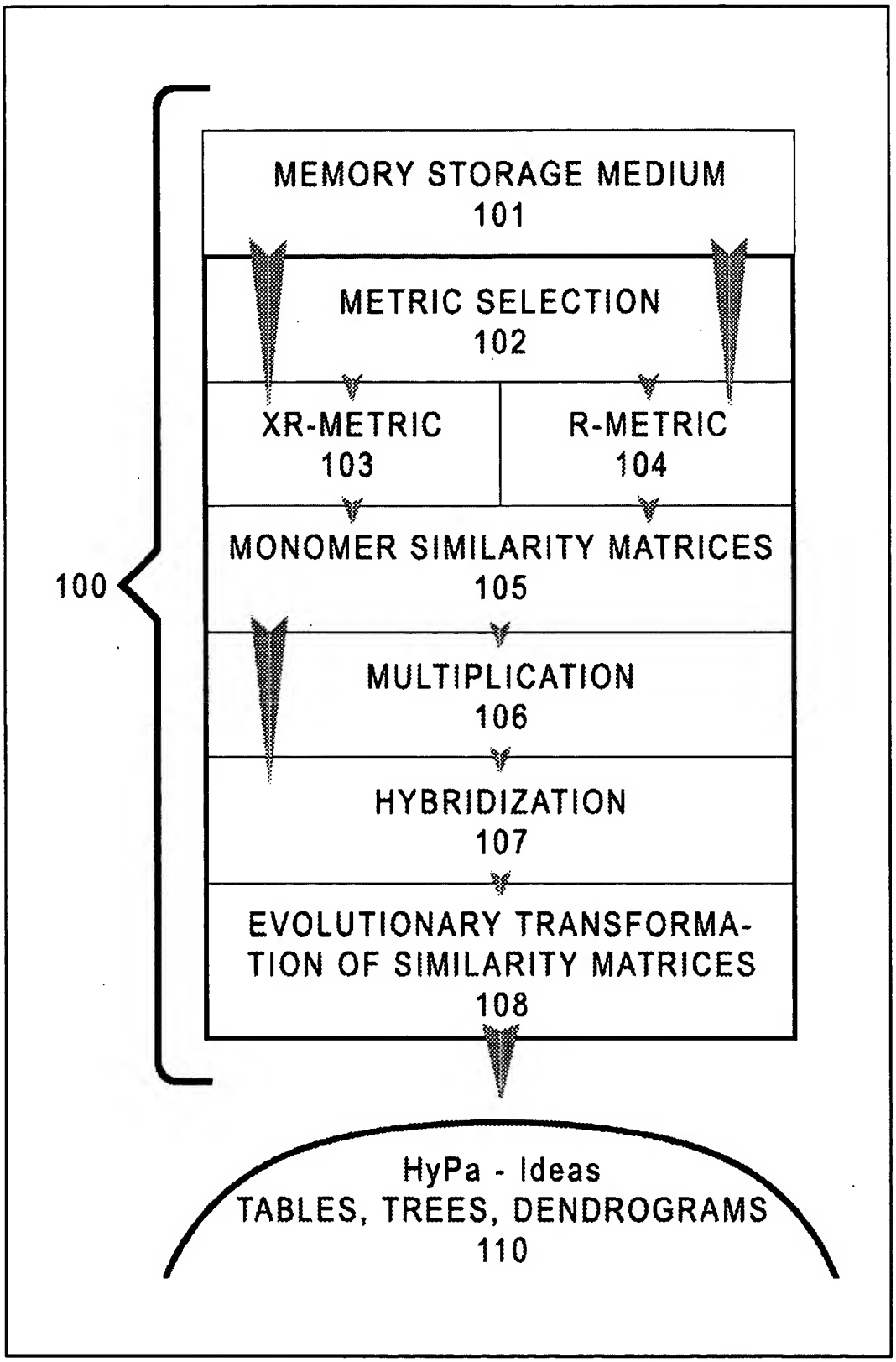

FIG. 1

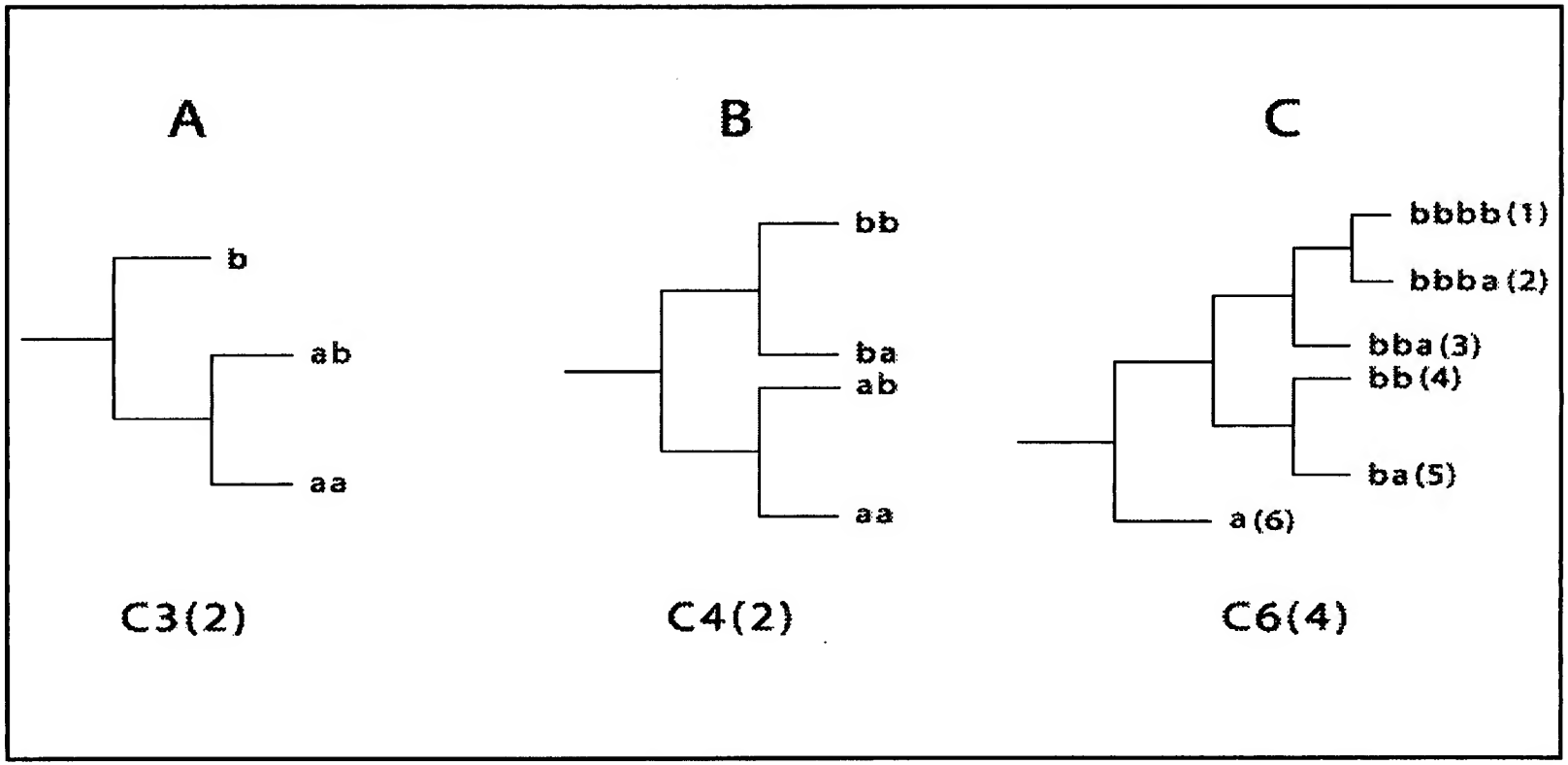

FIGS. 2A – 2C

Leonid Andreev, Dmitry Andreev
FIG. 3 of 43. A flow diagram of the method of this invention

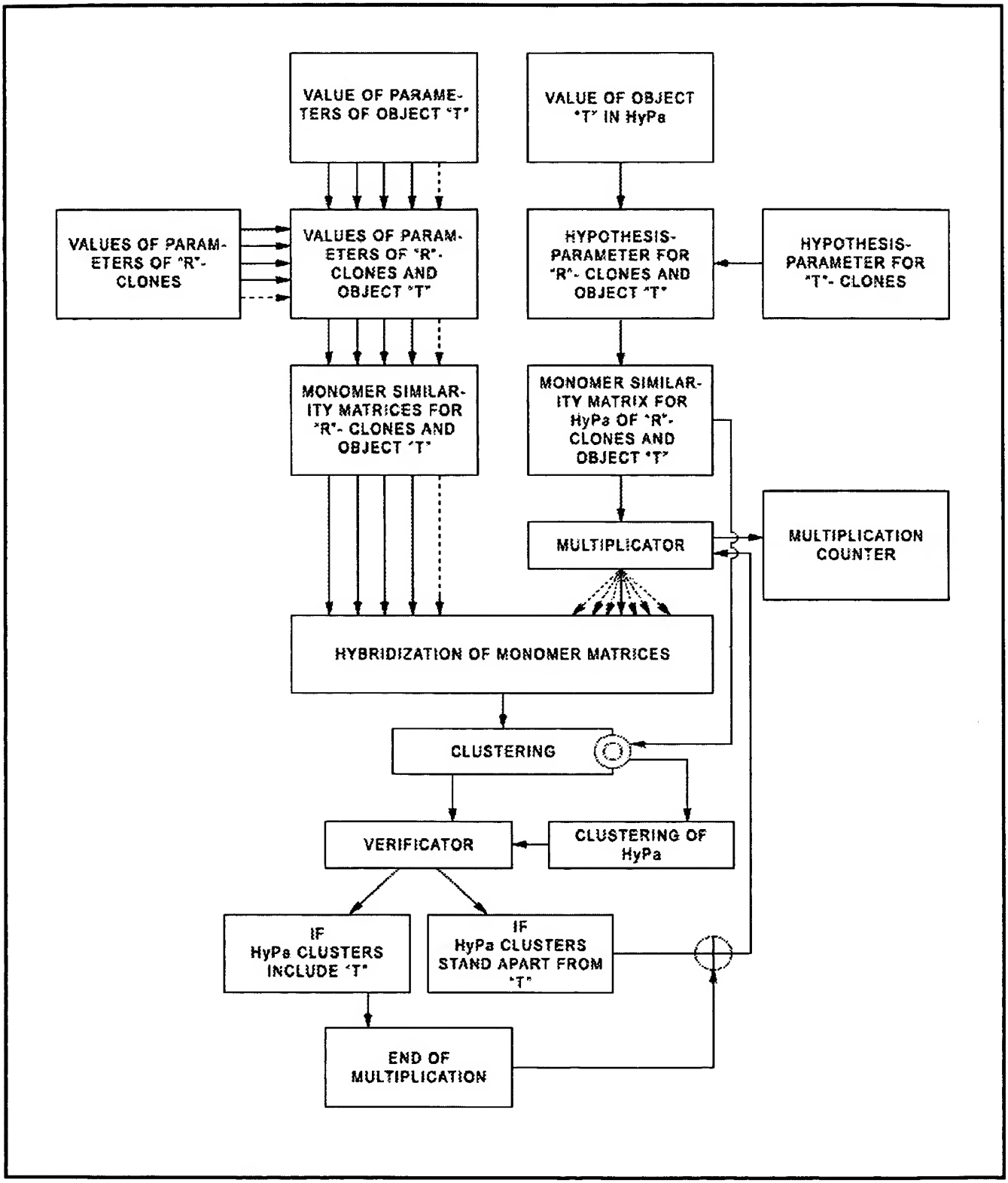

FIG. 3

Leonid Andreev, Dmitry Andreev. FIG. 4 of 43. Various kinds of trees resulting from clustering of a hypothesis-parameter

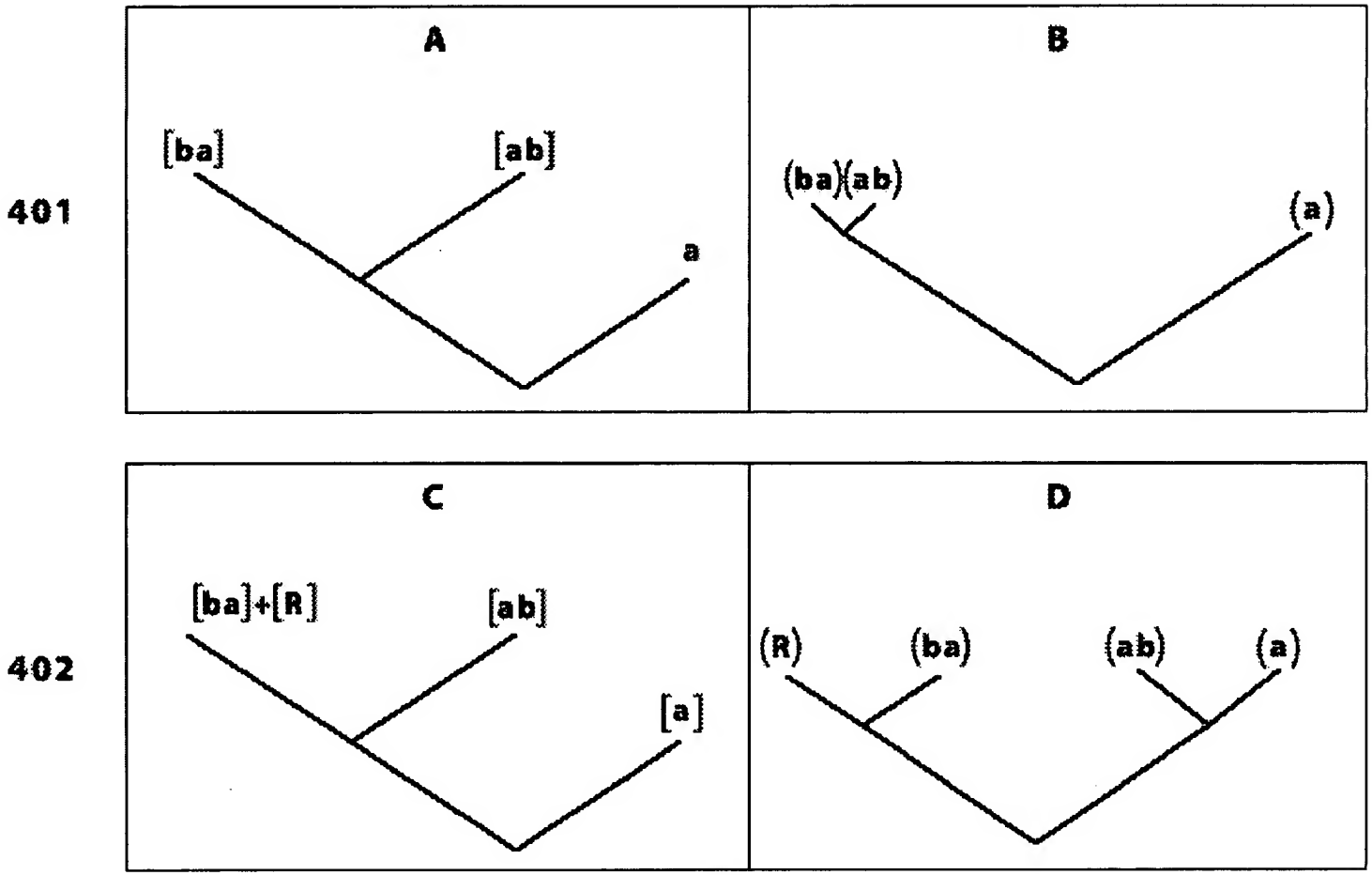

FIG. 4

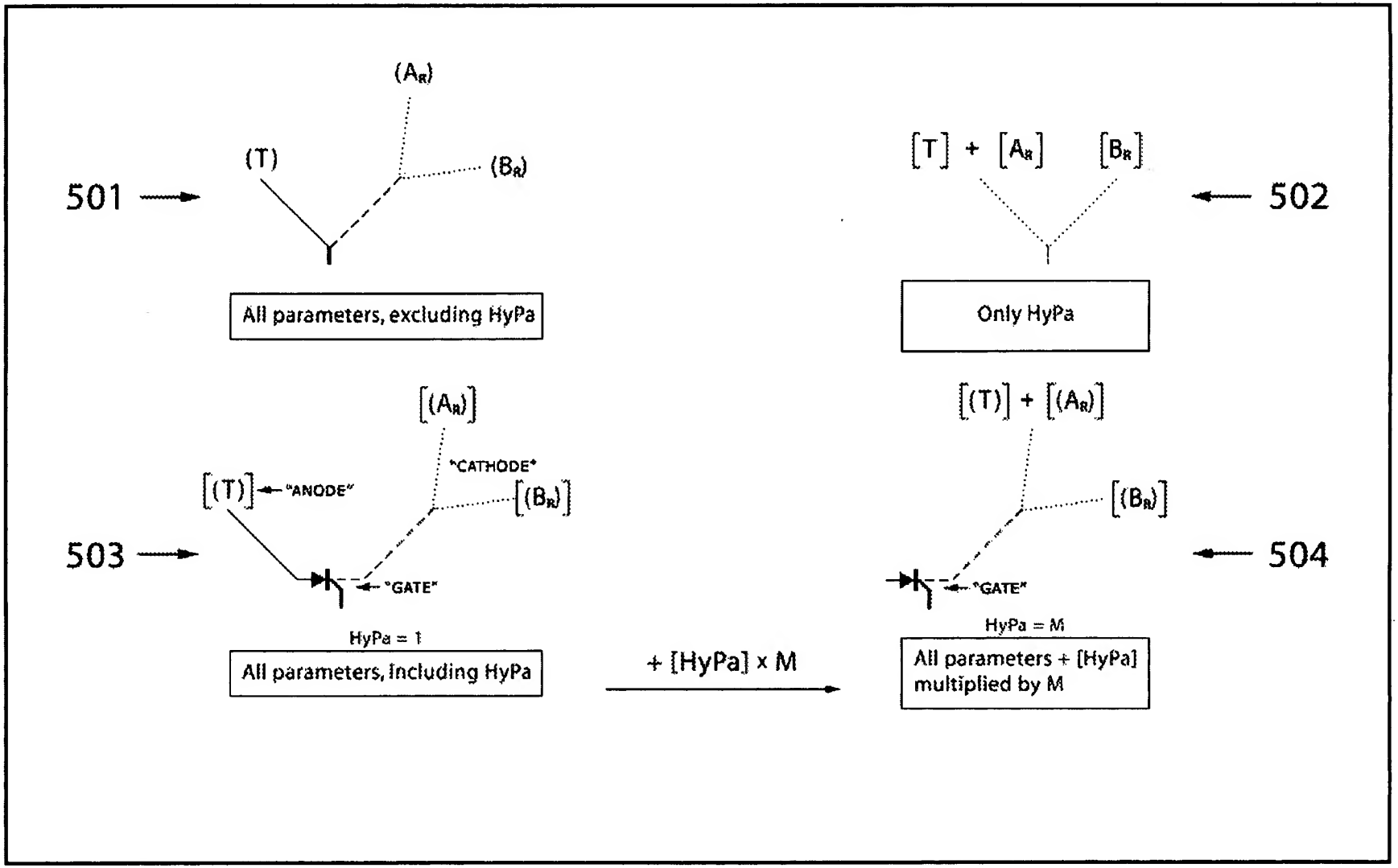
501
(A_R)
(T)
(B_R)
All parameters, excluding HyPa
502
[T] + [A_R]
[B_R]
Only HyPa
503
[(A_R)]
"CATHODE"
[(T)]
"ANODE"
[(B_R)]
"GATE"
HyPa = 1
All parameters, including HyPa
+ [HyPa] x M
504
[(T)] + [(A_R)]
[(B_R)]
"GATE"
HyPa = M
All parameters + [HyPa] multiplied by M

FIG. 5

Leonid Andreev, Dmitry Andreev
FIG. 6 of 43. 3D-diagrams of subclusters produced by clustering of 33 scattered points

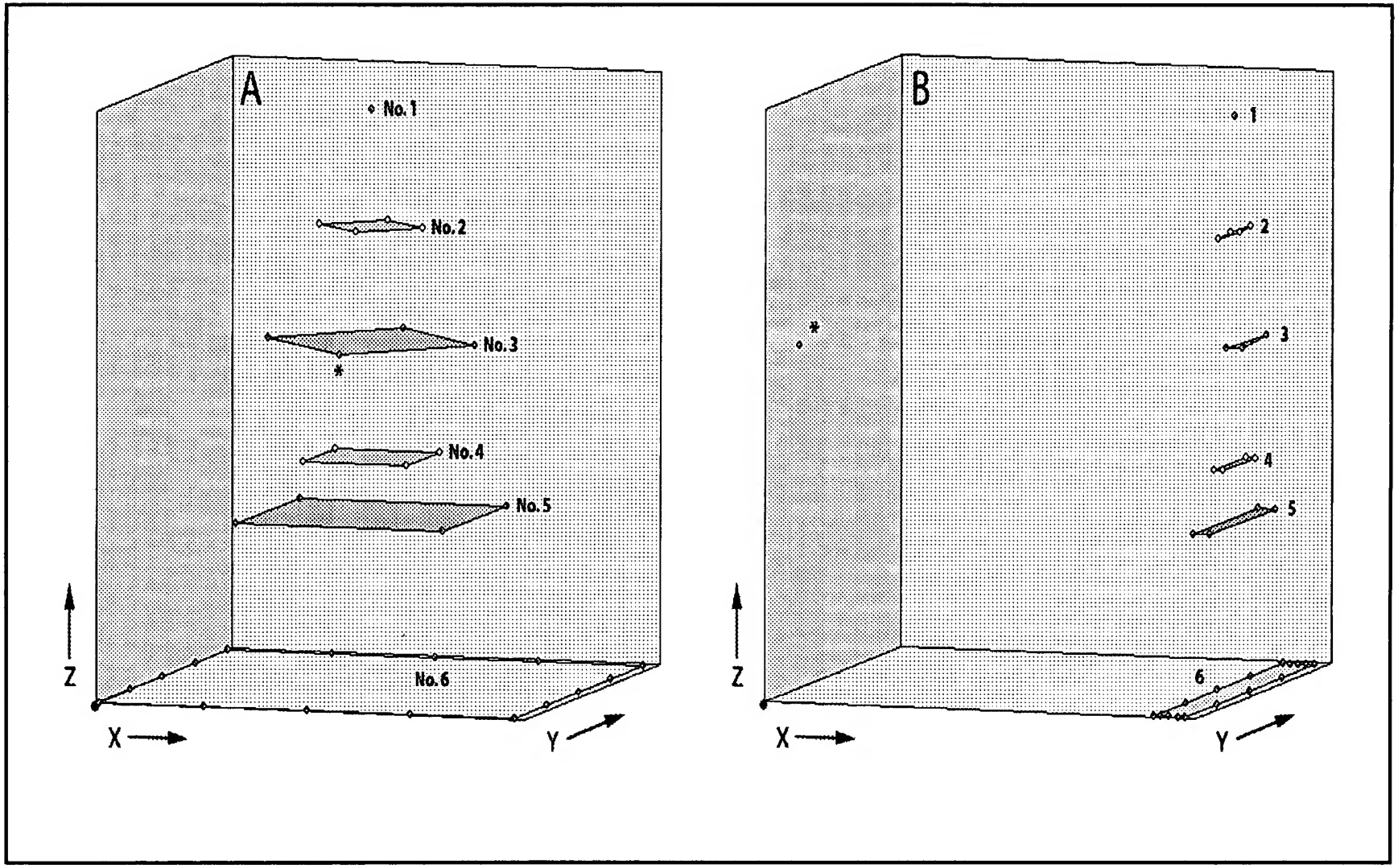

FIG. 6

Leonid Andreev, Dmitry Andreev.
FIG. 7 of 43. A plot showing changes in plausibility number *-ln M*

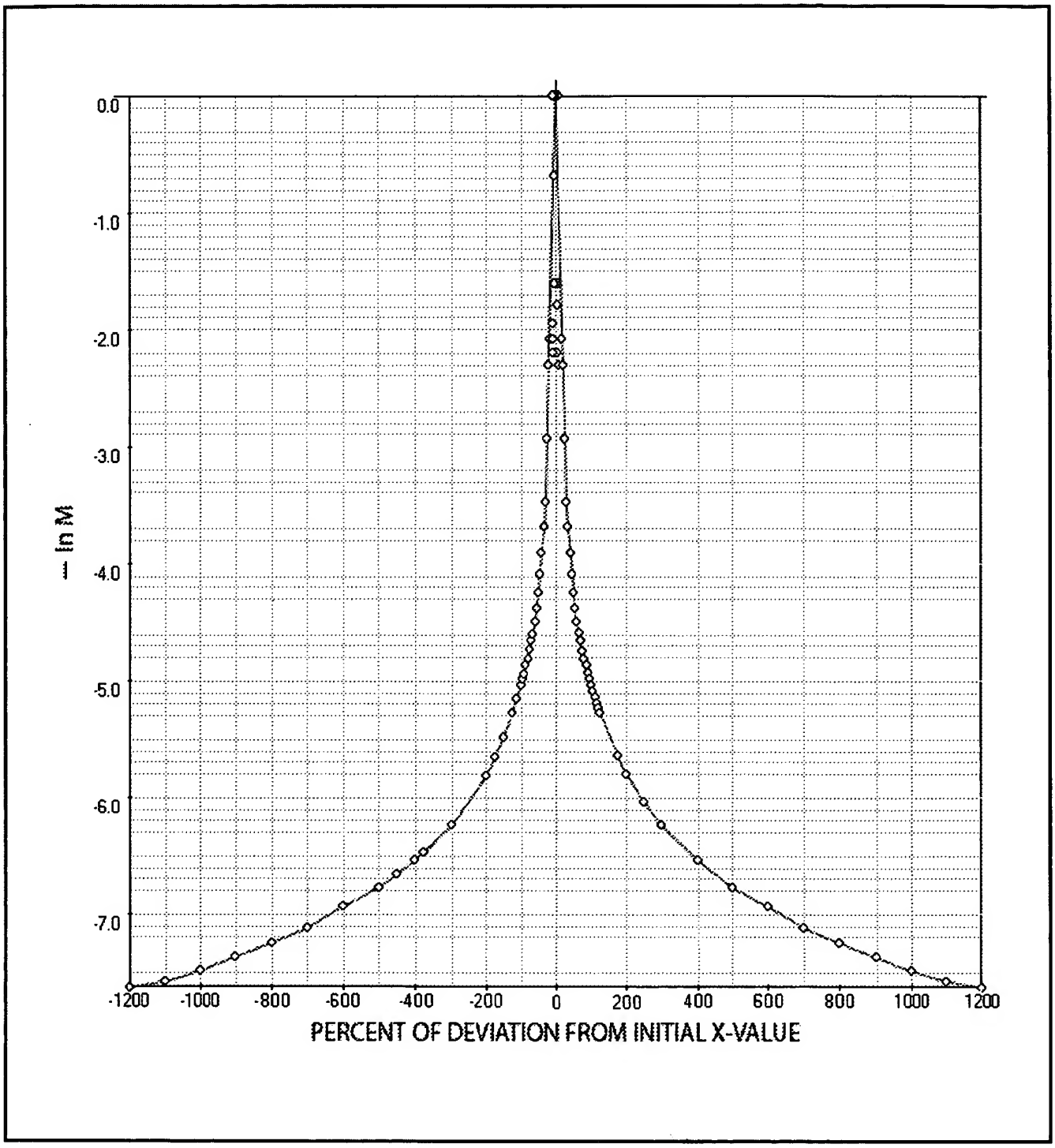

FIG. 7

Leonid Andreev, Dmitry Andreev

FIG. 8 of 43. Relationship between *ln* M_{ab} values for 245 cities of 50 states of the U.S.A. (reference object San Diego, CA)

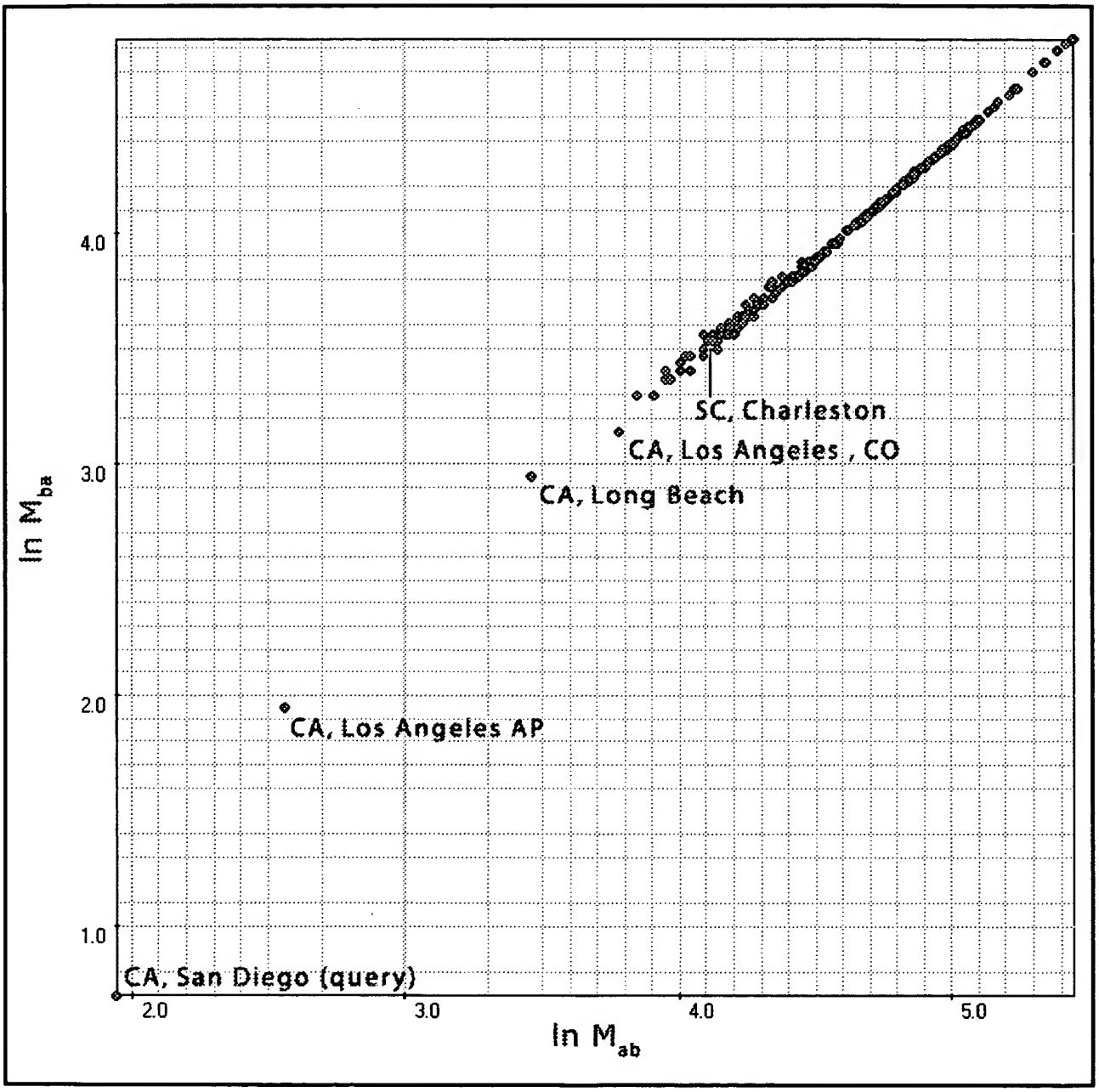

FIG. 8

Leonid Andreev, Dmitry Andreev

FIG. 9 of 43. Relationship between *ln* M_{ab} values for 245 cities of 50 states of the U.S.A. (reference objects San Diego, CA, and Charleston, SC)

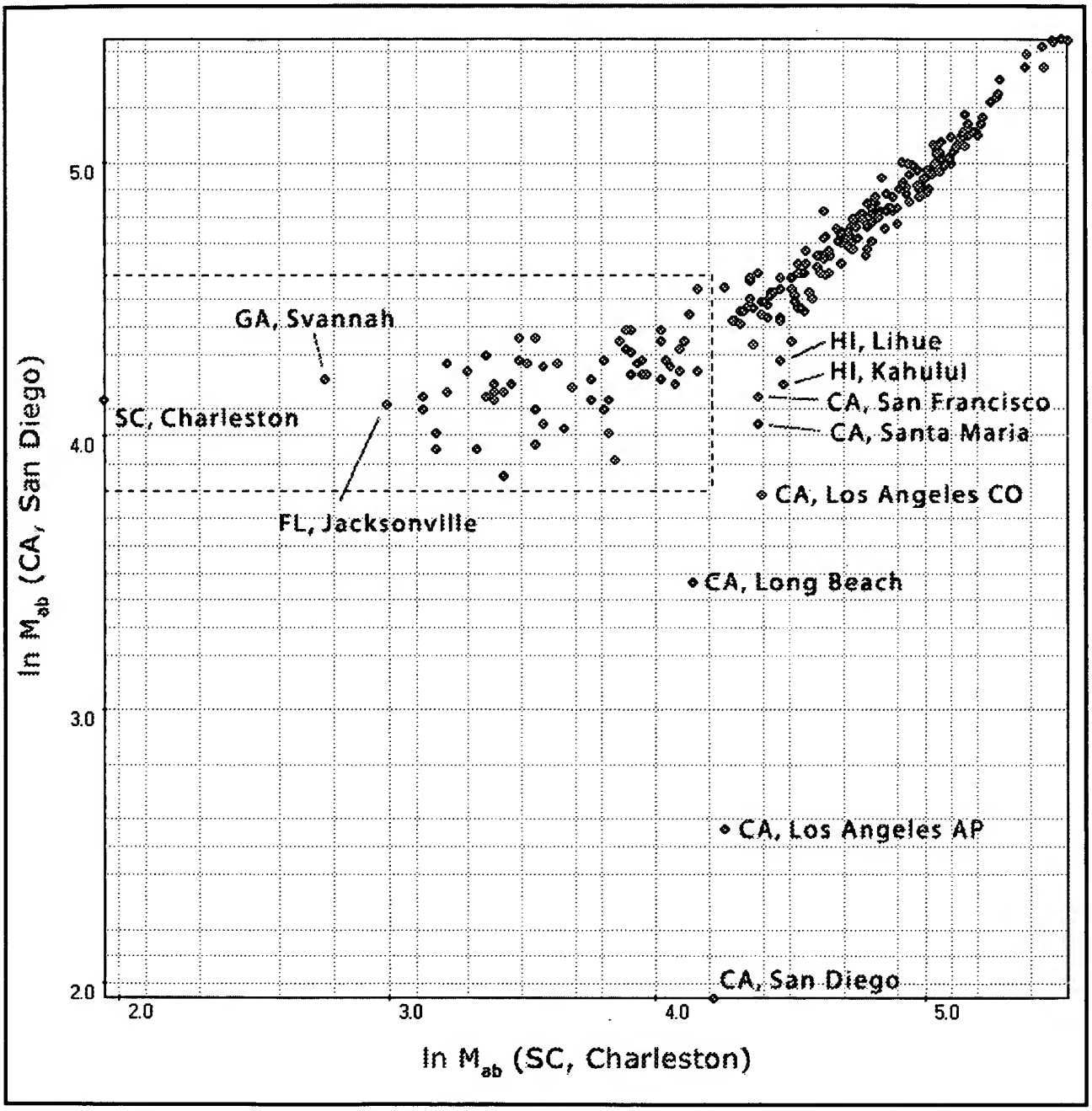

FIG. 9

Leonid Andreev, Dmitry Andreev
FIG. 10 of 43. 3D-diagram of grouping of 80 countries (51 demographic parameters) based on implausibility numbers (*ln M*)

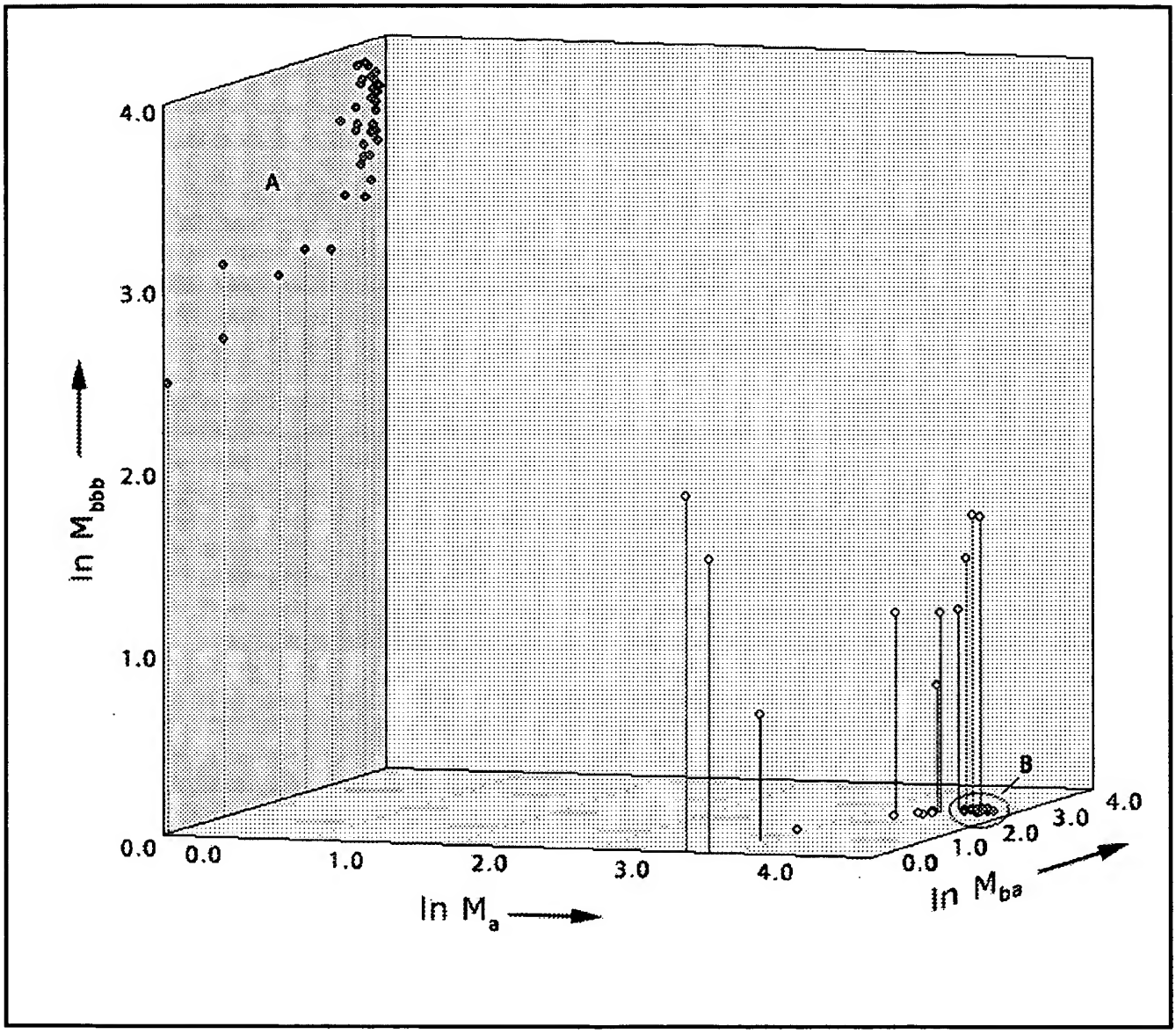

FIG. 10

FIG. 11 of 43. 3D-diagram of grouping of 80 countries, using 51 demographic parameters and based on implausibility numbers (*ln M*).

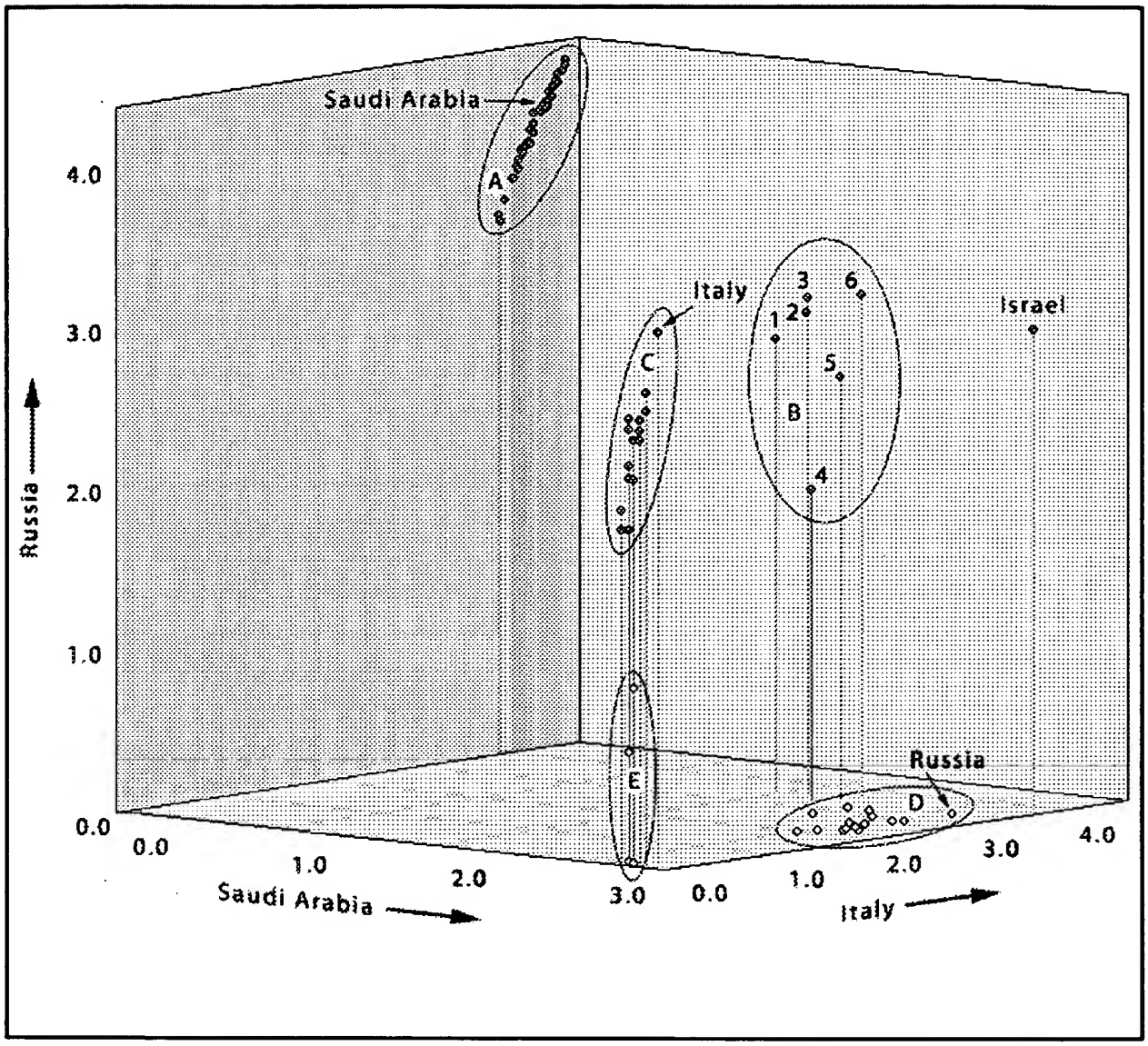

FIG. 11

Leonid Andreev, Dmitry Andreev

FIG. 12 of 43. 3D-diagram of grouping of 74 countries, using 51 demographic parameters and based on implausibility numbers (*ln M*).

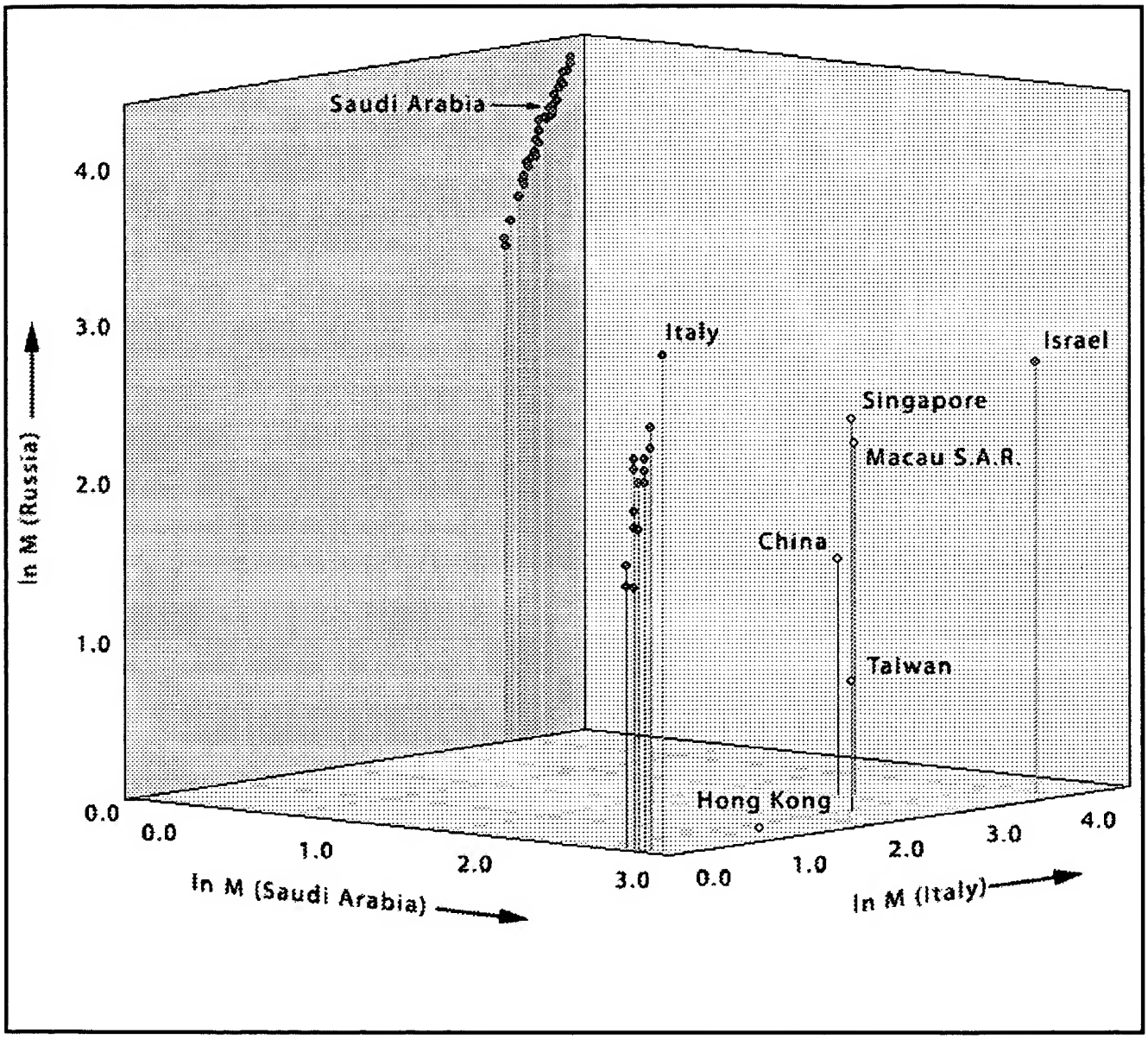

FIG. 12

FIG. 13 of 43. Clustering by evolutionary transformation of a similarity matrix based on 4 different multiplication number values

1.1.1. Hong Kong 1.1.2. China Macau S.A.R. Singapore Taiwan.	1.2.1. Austria Belgium Denmark Germany Greece Norway Sweden Switzerland UK. 1.2.2. Finland France Italy Luxembourg Netherlands Portugal Spain.	2.1. India	2.2.1. Algeria Bahrain Egypt Libya Morocco 2.2.2. Djibouti Iraq Jordan Kuwait Oman Qatar Saudi Arabia Syria United Arab Emir. West Bank Yemen

FIG. 13

FIG. 14 of 43. A plot showing the relationship between multiplication numbers M(2) and M(3) computed for 17 countries described by 34 parameters based on population pyramids.

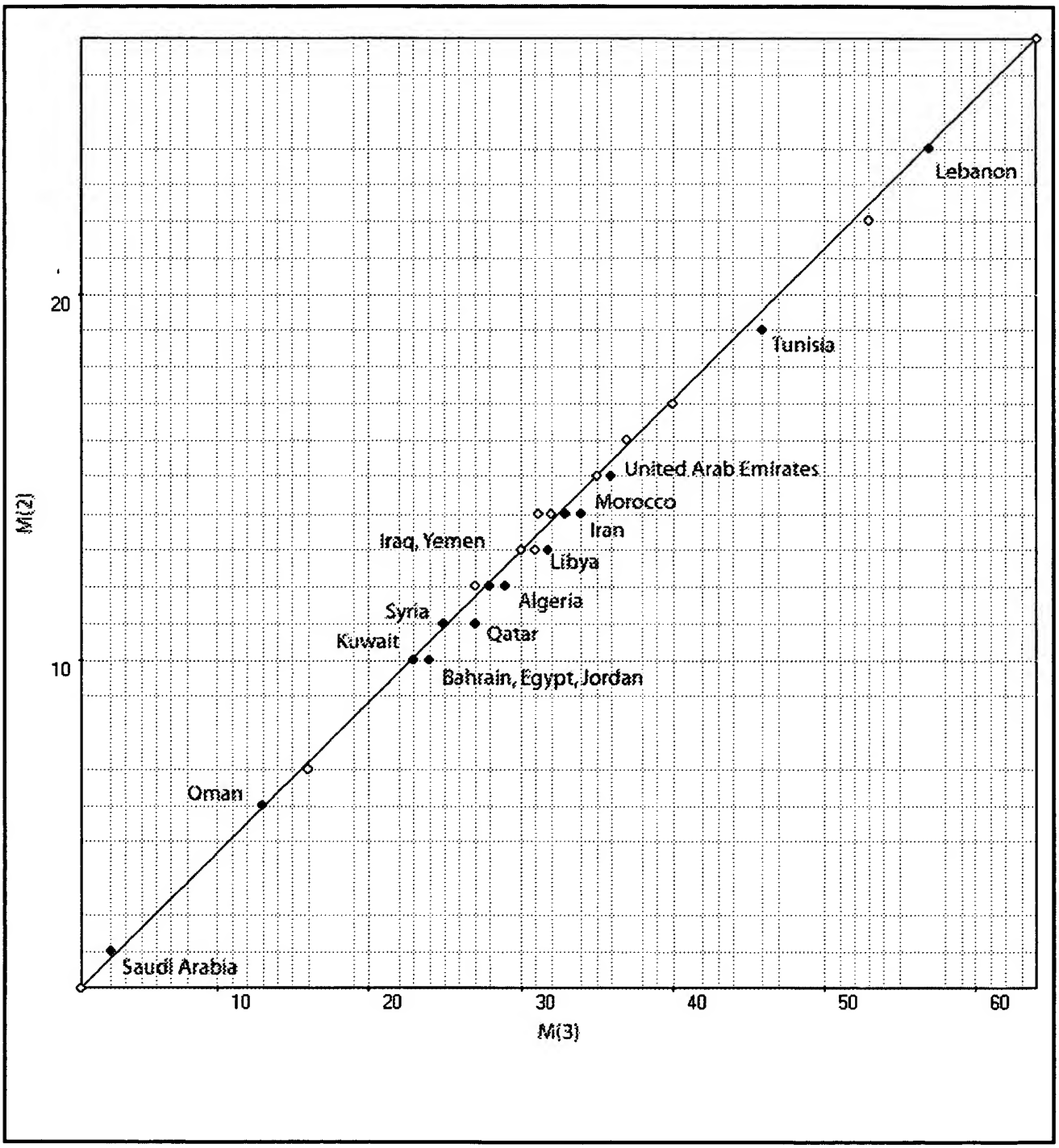

FIG. 14

Leonid Andreev, Dmitry Andreev. FIGS. 15A – 15B of 43. Correlation between implausibility numbers and demographic parameters of 220 countries under analysis

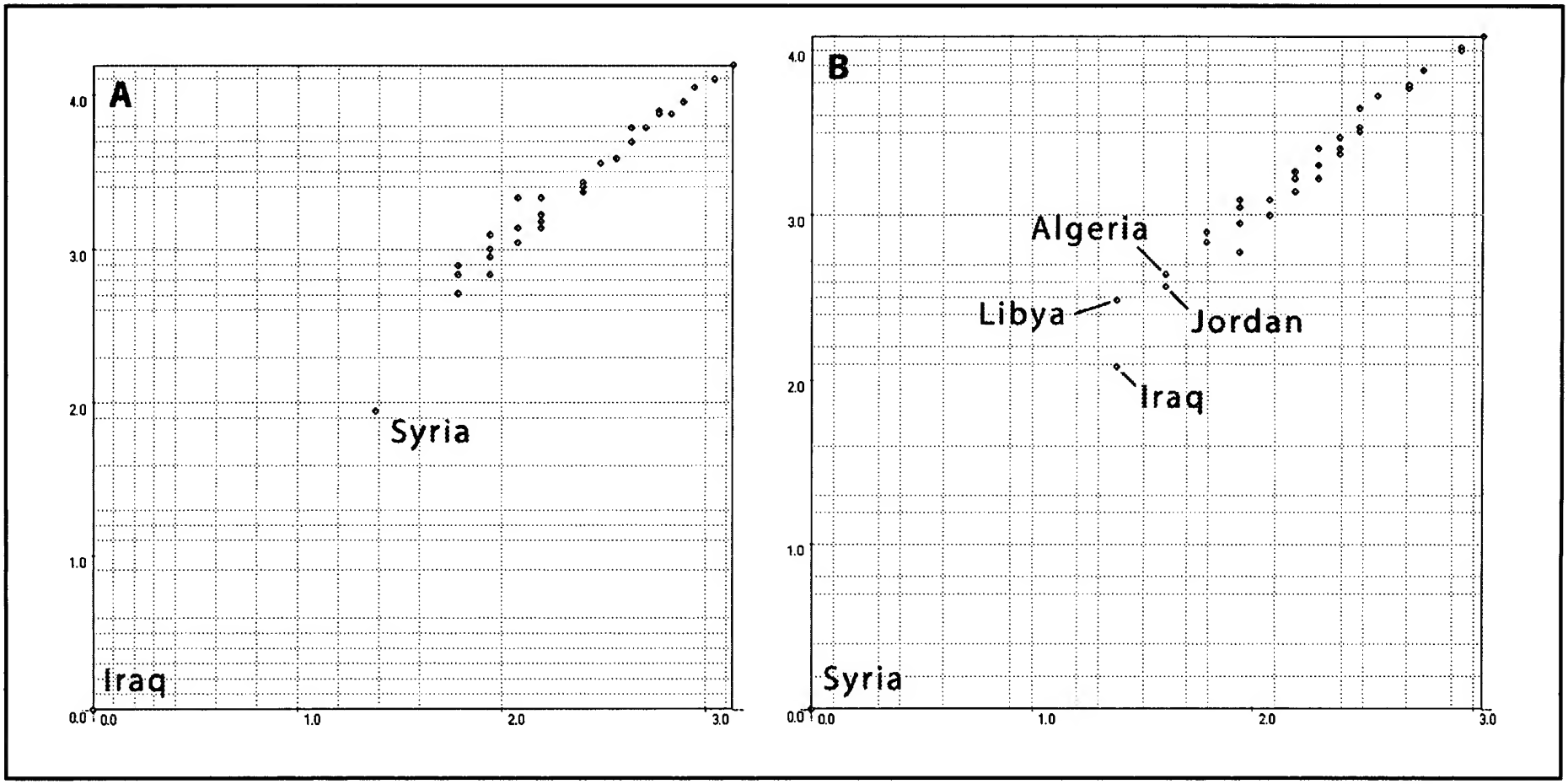

FIGS. 15A – 15B

FIGS. 15C – 15D of 43. Illustrations of searches for closest analogs of Jordan and Kuwait as reference objects.

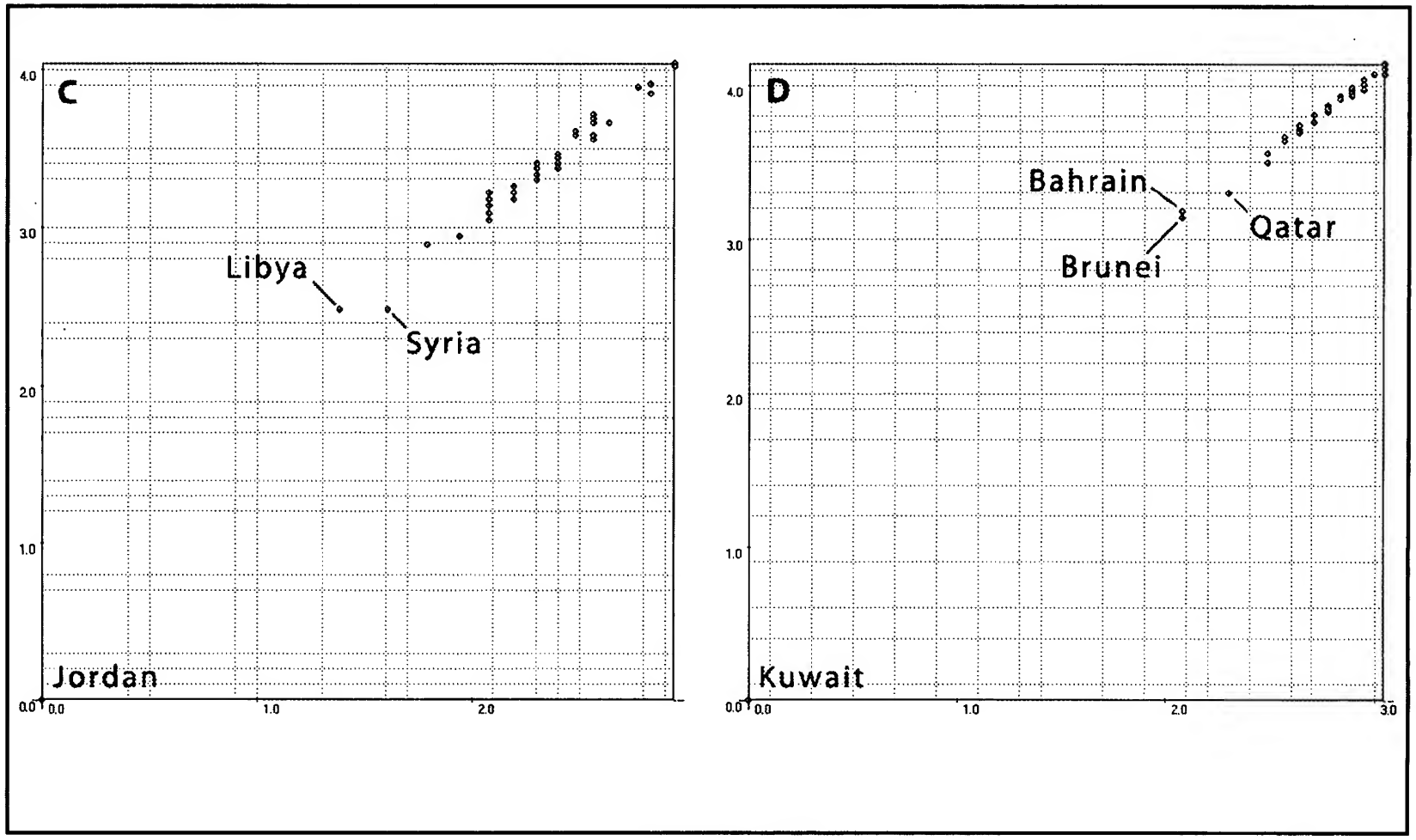

FIGS. 15C – 15D

Leonid Andreev, Dmitry Andreev
FIGS. 15E – 15F of 43. Illustrations of searches for closest analogs of Qatar and United Arab Emirates as reference objects.

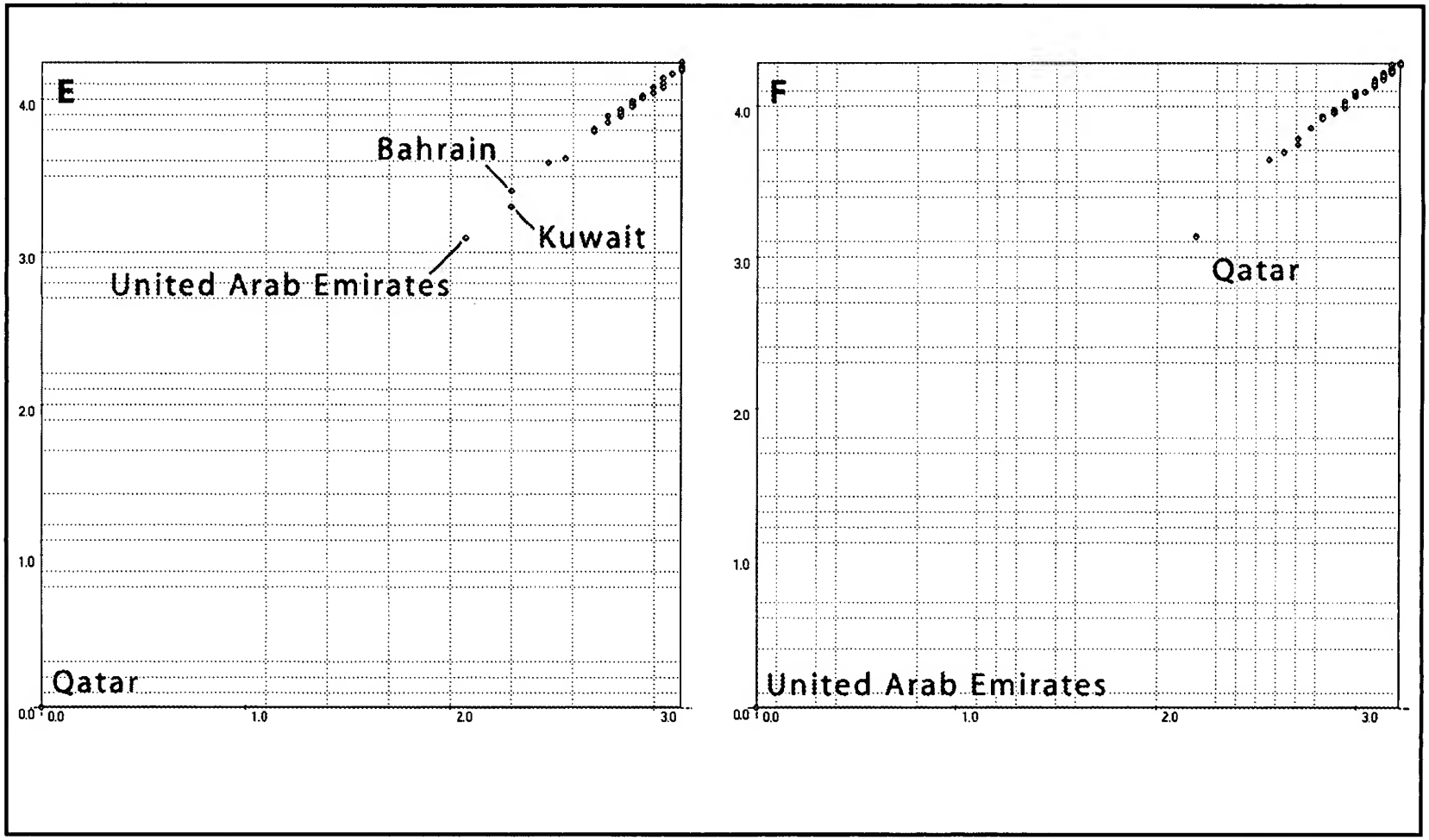

FIGS. 15E – 15F

Leonid Andreev, Dmitry Andreev. FIG. 16 of 43. A plot-map of 220 countries, based on 34 parameters of population pyramids, using Russia and Saudi Arabia as reference objects

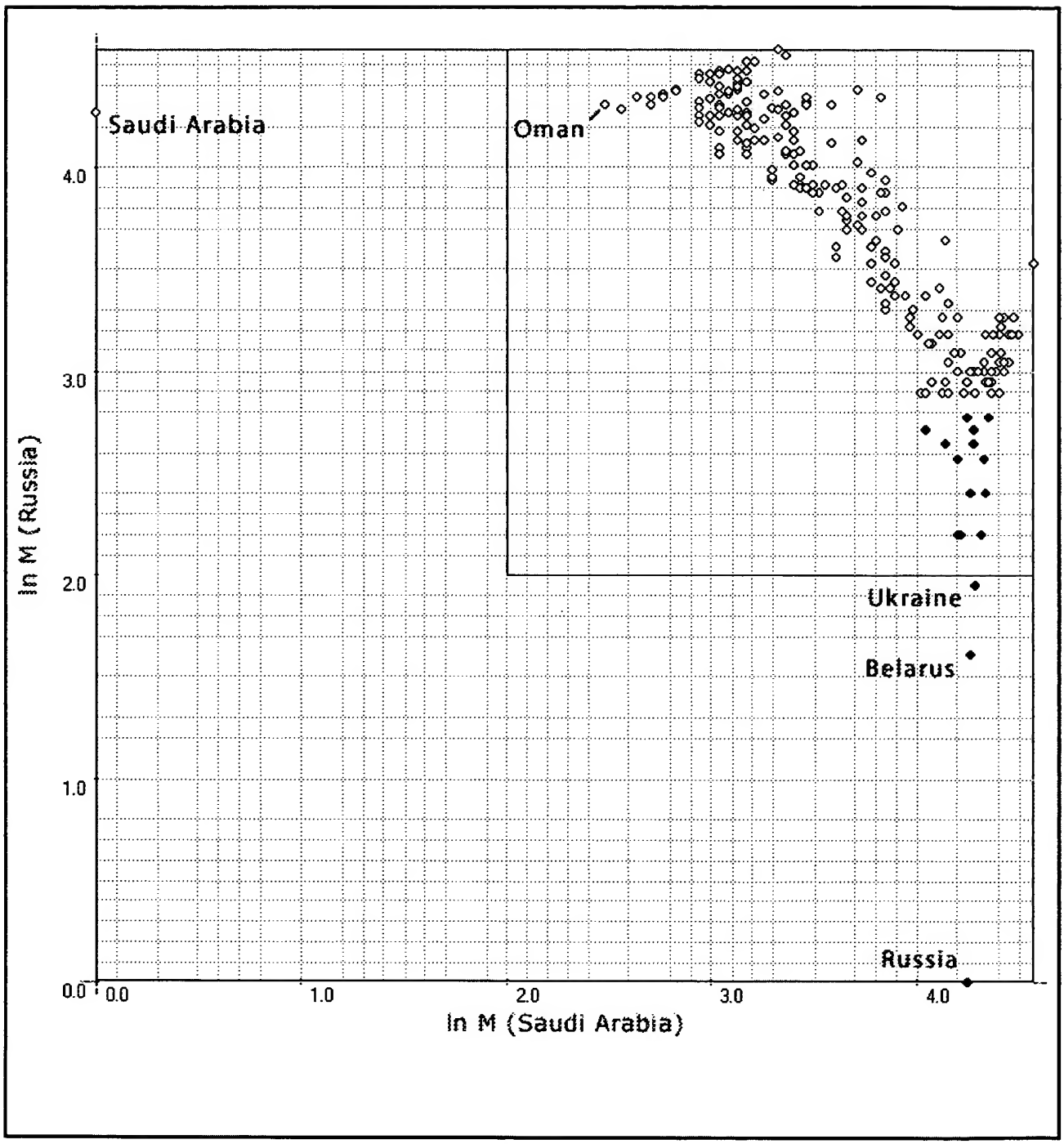

FIG. 16

FIG. 17 of 43. Schematic image of a human body referred to in the example on HyGV application in image and gait recognition

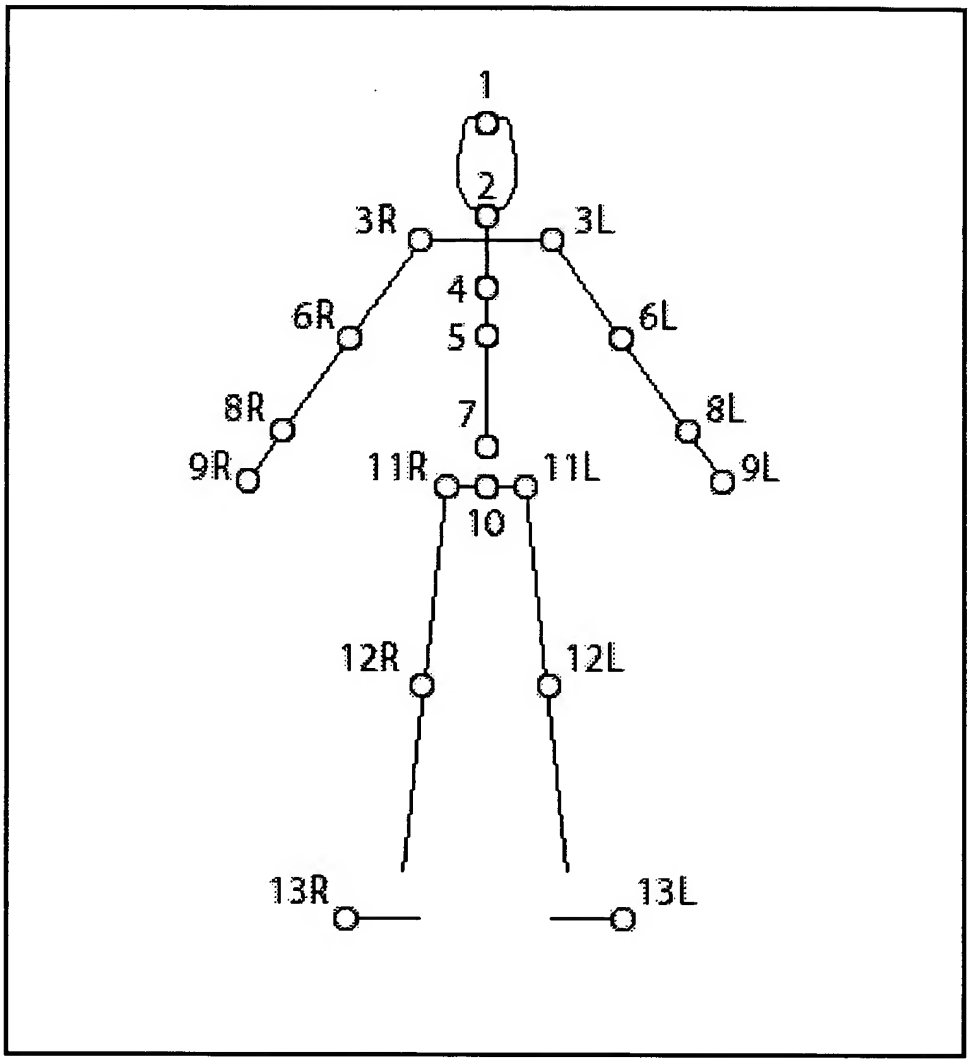

FIG. 17

Leonid Andreev, Dmitry Andreev
FIG. 18 of 43. 42 out of 75 artificially generated images of human body poses used in the example of HyGV application in image recognition

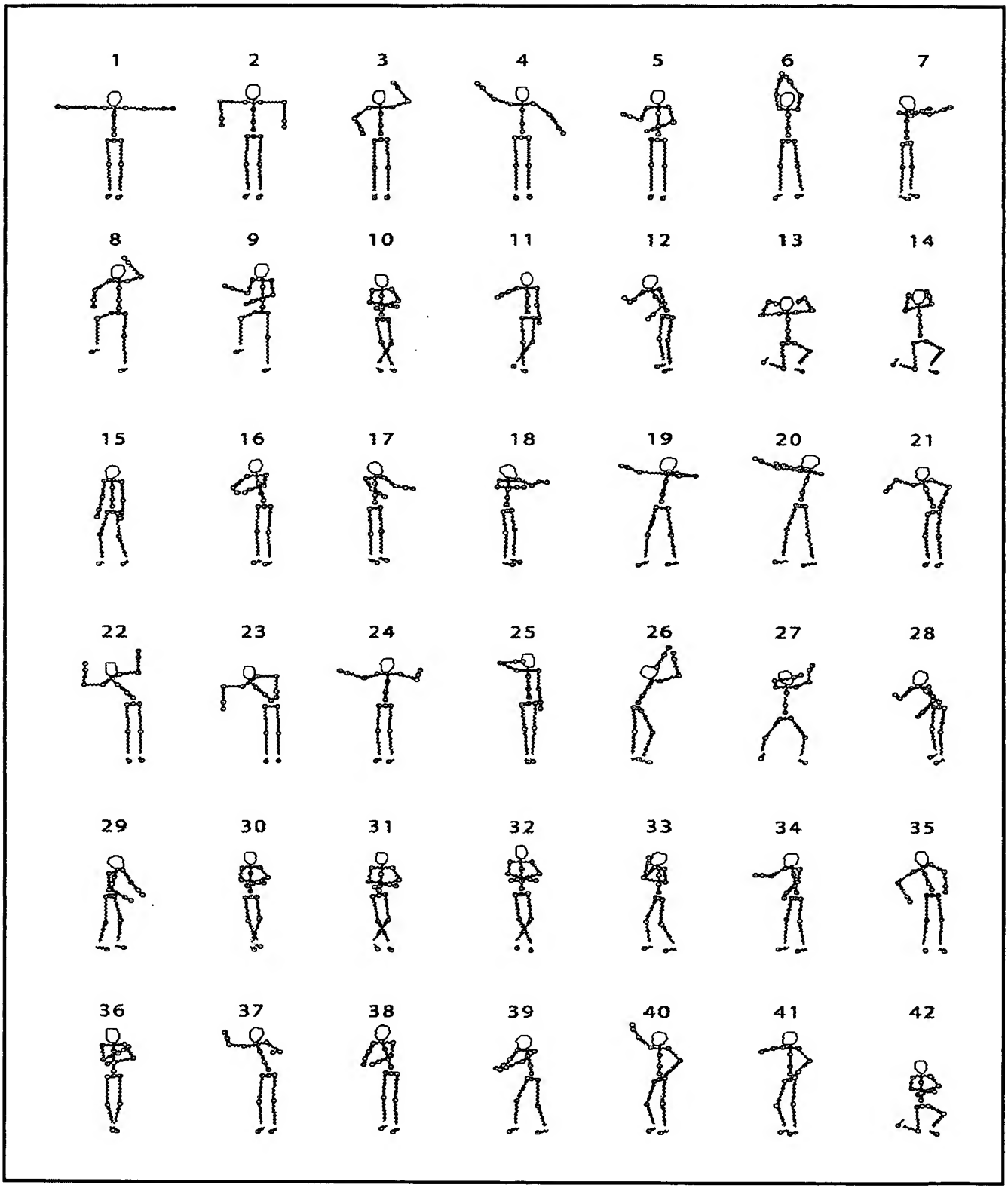

FIG. 18

Leonid Andreev, Dmitry Andreev. FIG. 19 of 43. Search for closest analogs of images of human body poses in a database of 75 images, by the HyGV-CC method

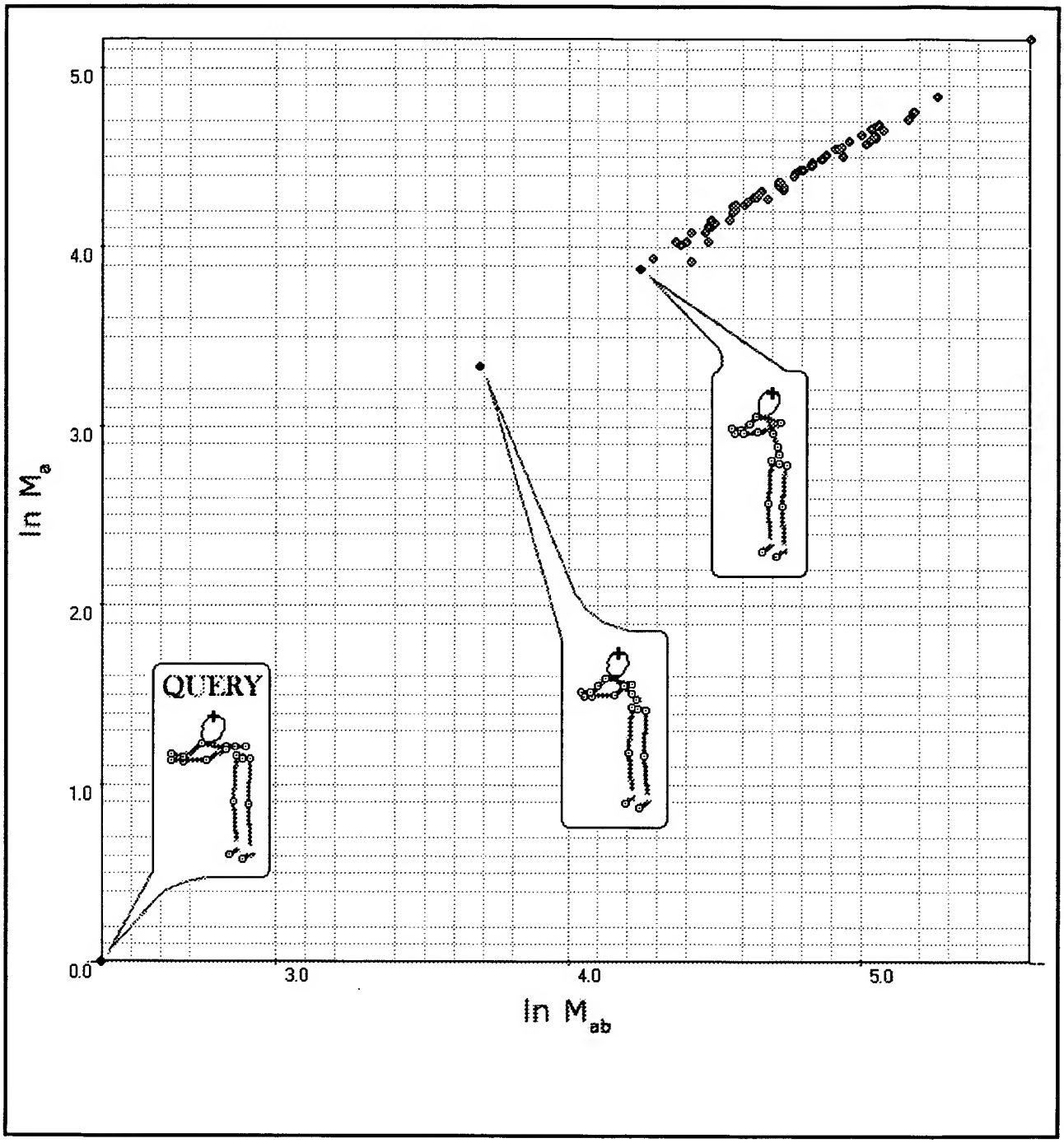

FIG. 19

Leonid Andreev, Dmitry Andreev. FIG. 20 of 43. Search (among 75 images) for closest analogs of a human body pose with hands up and legs straight

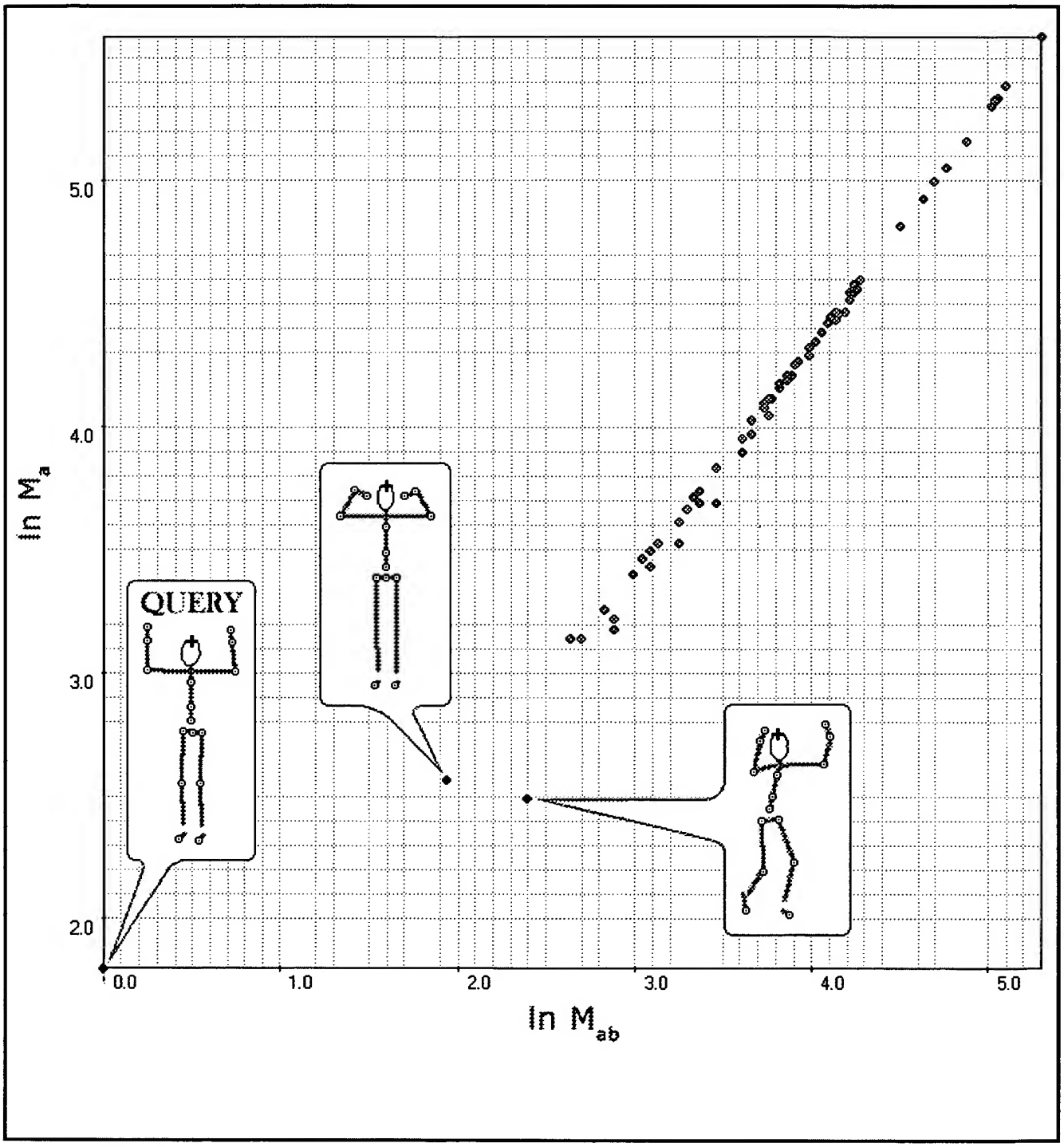

FIG. 20

Leonid Andreev, Dmitry Andreev. FIG. 21 of 43. Search (among 75 images) for closest analogs of a human body pose with the right leg and right hand raised

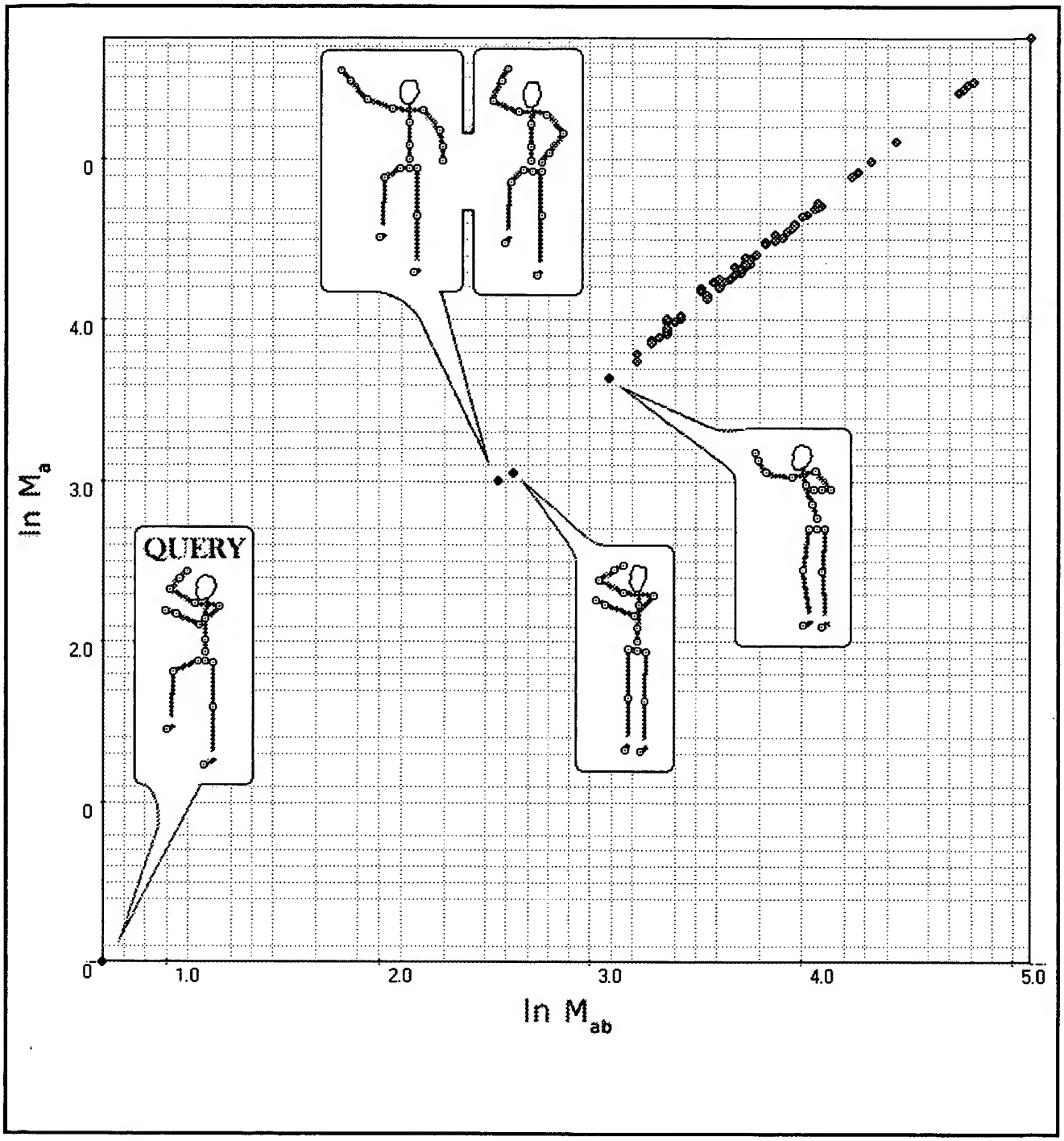

FIG. 21

Leonid Andreev, Dmitry Andreev. FIG. 22 of 43. Search (among 75 images) for closest analogs of a human body pose with hands down and legs straight

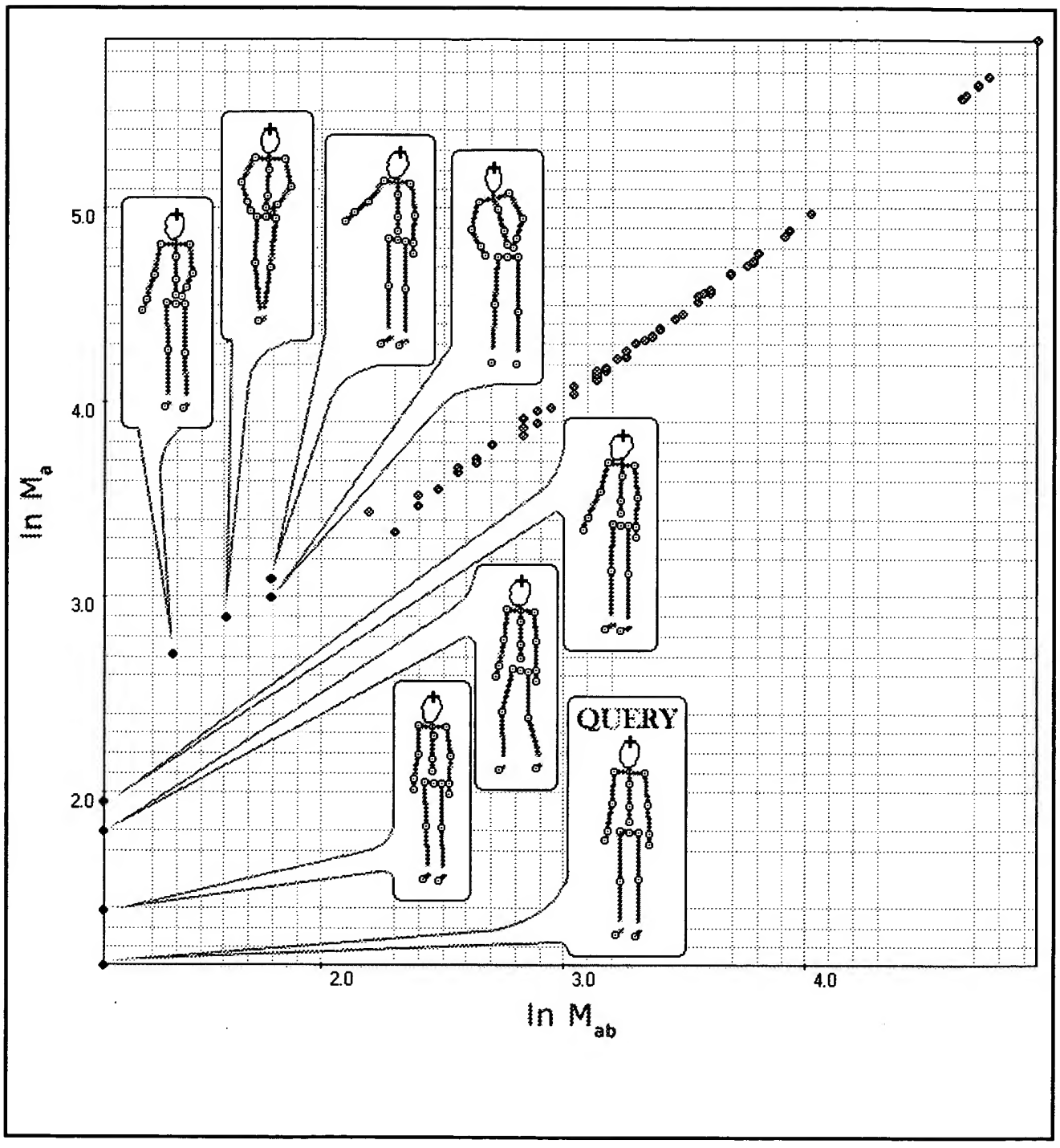

FIG. 22

Leonid Andreev, Dmitry Andreev. FIG. 23 of 43. Search (among 75 images) for closest analogs of a human body in a sitting position

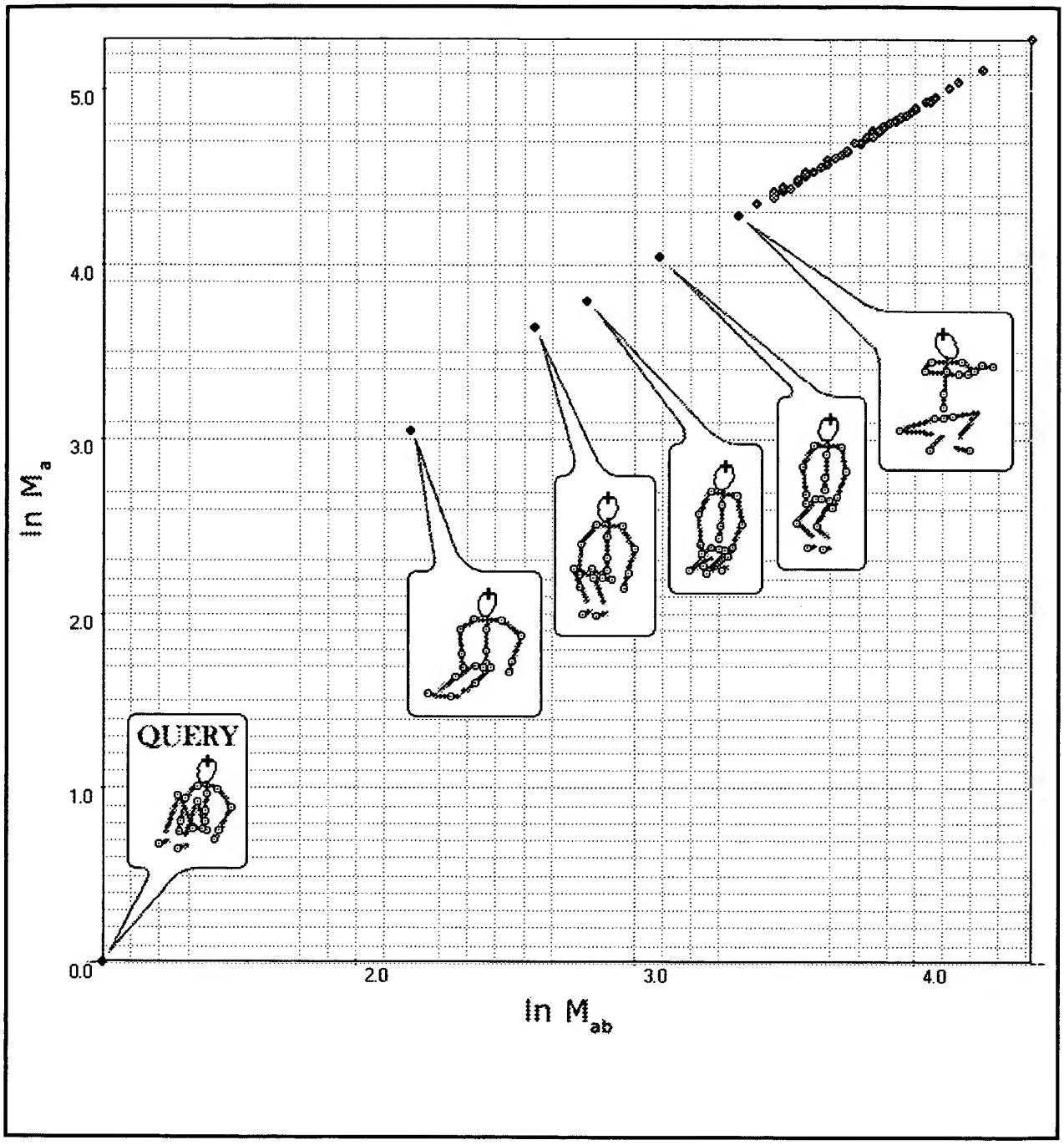

FIG. 23

FIG. 24 of 43. The result of search (among 75 images) for closest analogs of a human body lying on the stomach

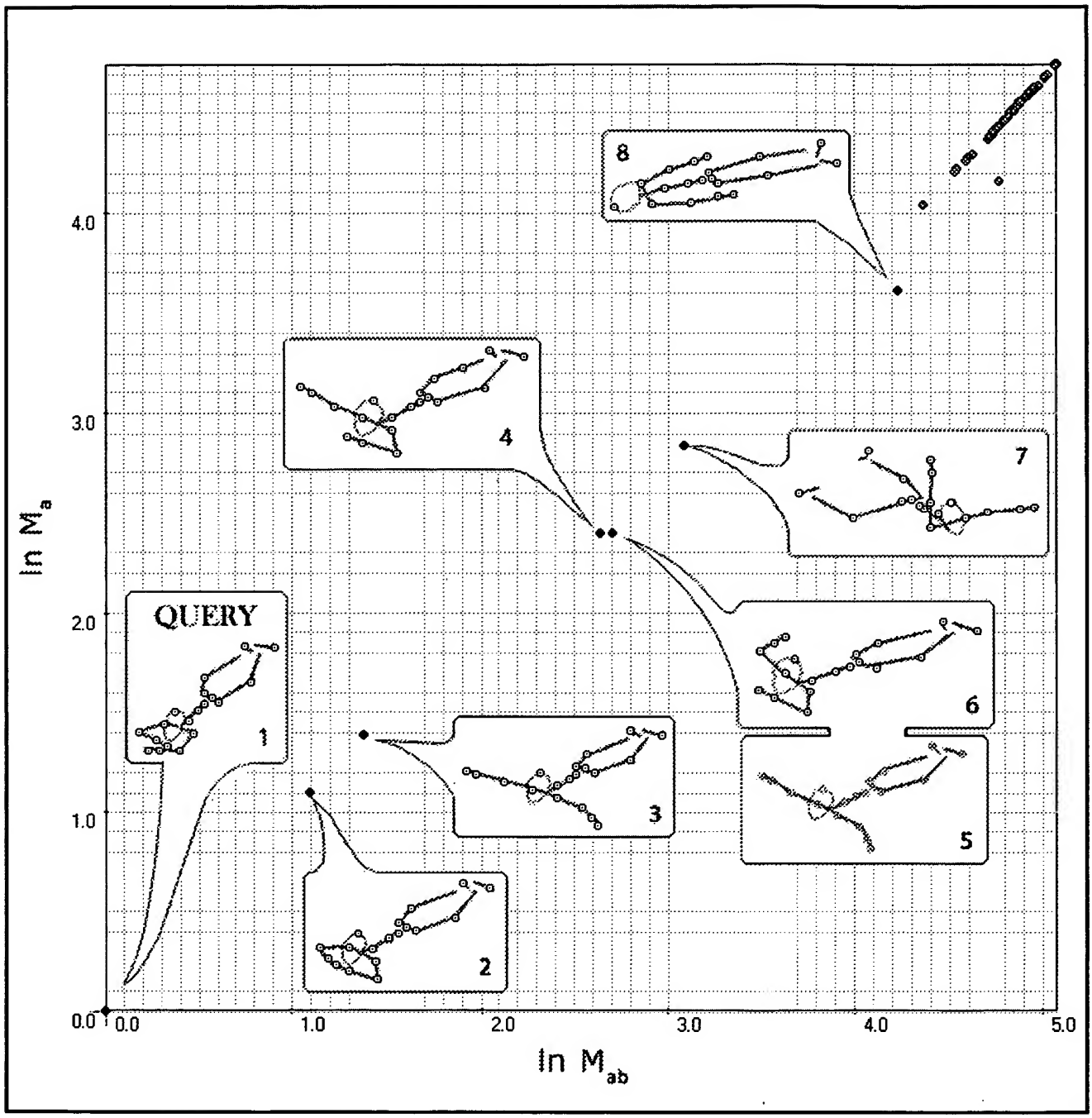

FIG. 24

Leonid Andreev, Dmitry Andreev

FIG. 25 of 43. Relationship between similarity coefficients S_a and S_{ab} computed by equation 6 for a human body pose shown in FIG. 24

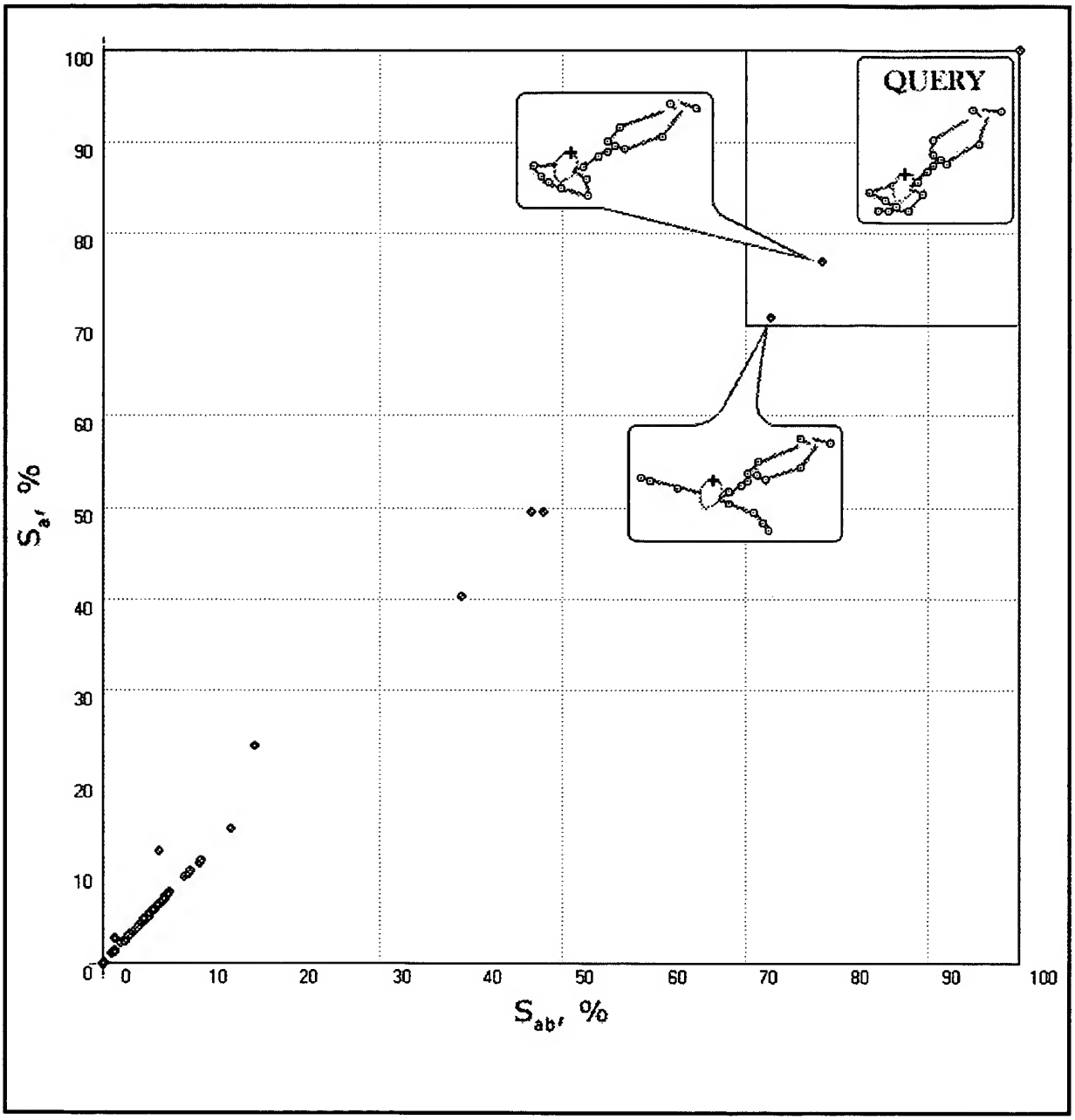

FIG. 25

Pose number in FIG. 17	Number of multiplications (capsule of clones for a query illustrated in FIG. 18-23)							
	Whole figure[1,2]	Left side[3]	Right side[4]	Torso center[5]	Left calf	Right calf	Left fingers, forearm and hand	Right fingers, forearm and hand
1	121/121	59	47	24	14	13	5	4
1	139/139	59	56	24	14	13	14	13
3	133/133	59	49	25	14	13	5	19
4	139/139	64	51	24	14	13	20	7
5	141/141	63	54	24	14	13	19	10
6	139/139	55	59	25	14	13	12	16
7	117/116	47	45	24	14	13	3	3
8	122/121	48	49	24	14	8	6	16
9	130/131	64	43	21	14	8	19	10
14	141/141	60	57	24	14	13	17	10
11	145/145	66	59	24	14	13	26	9
12	130/130	59	45	21	13	12	20	8
13	99/99	25	41	33	9	13	3	3
14	99/99	34	41	24	9	13	3	3

[1] described by 18 parameters.
[2] first number in each pair indicates an experimentally established number of multiplications, second number is a total of multiplications for "left half", "right half" and "torso center".
[3] described by 7 parameters
[4] described by 7 parameters
[5] described by 4 parameters

FIG. 26

Leonid Andreev, Dmitry Andreev
FIG. 27 of 43. 45 artificially generated schematic images ("frames") of a human figure in the process of walking, referred to in the example of HyGV application in gait recognition

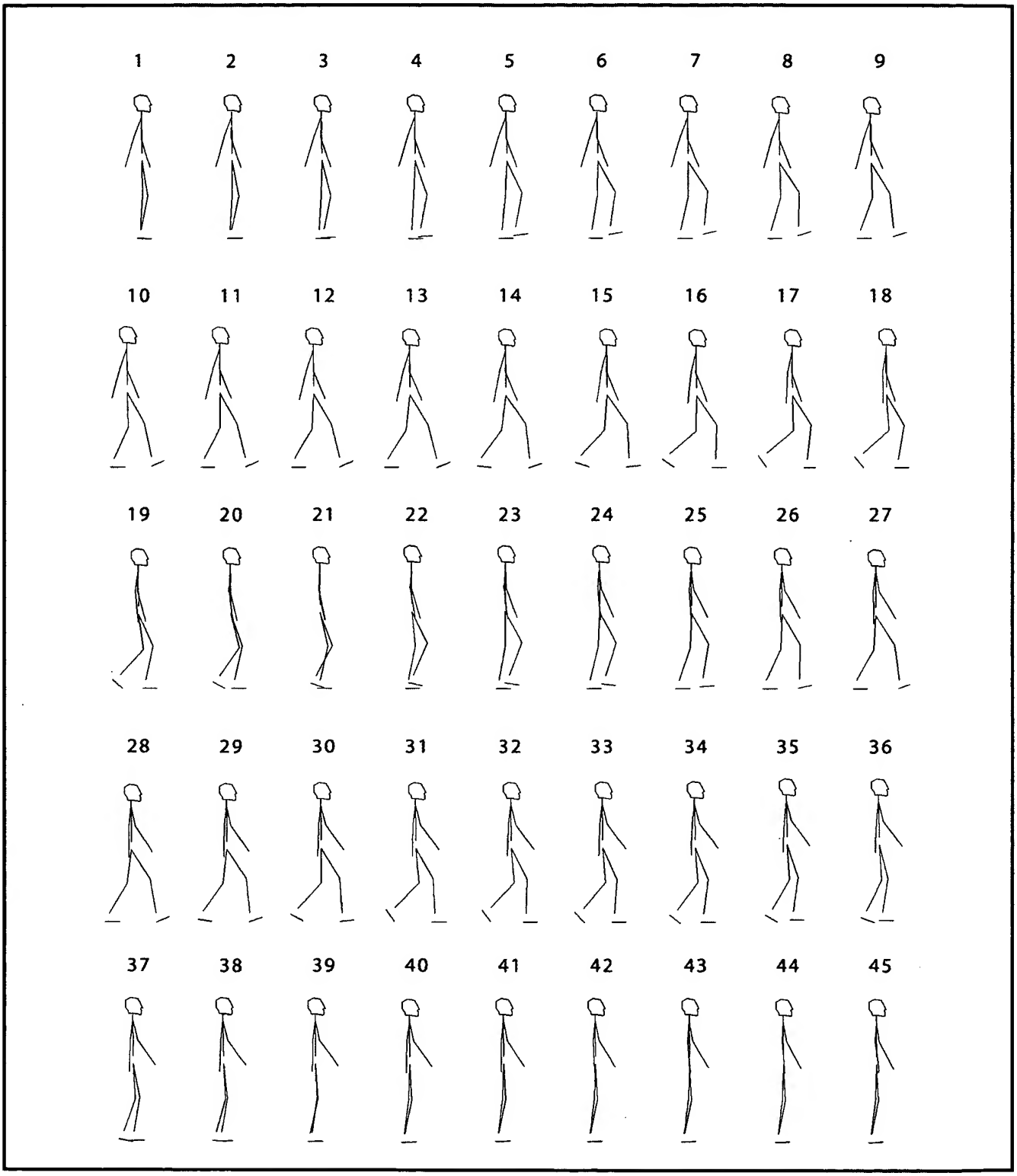

FIG. 27

Leonid Andreev, Dmitry Andreev. FIG. 28 of 43. A plot showing the multiplication number (M) changes in accordance with the walking motion frames shown in FIG. 27

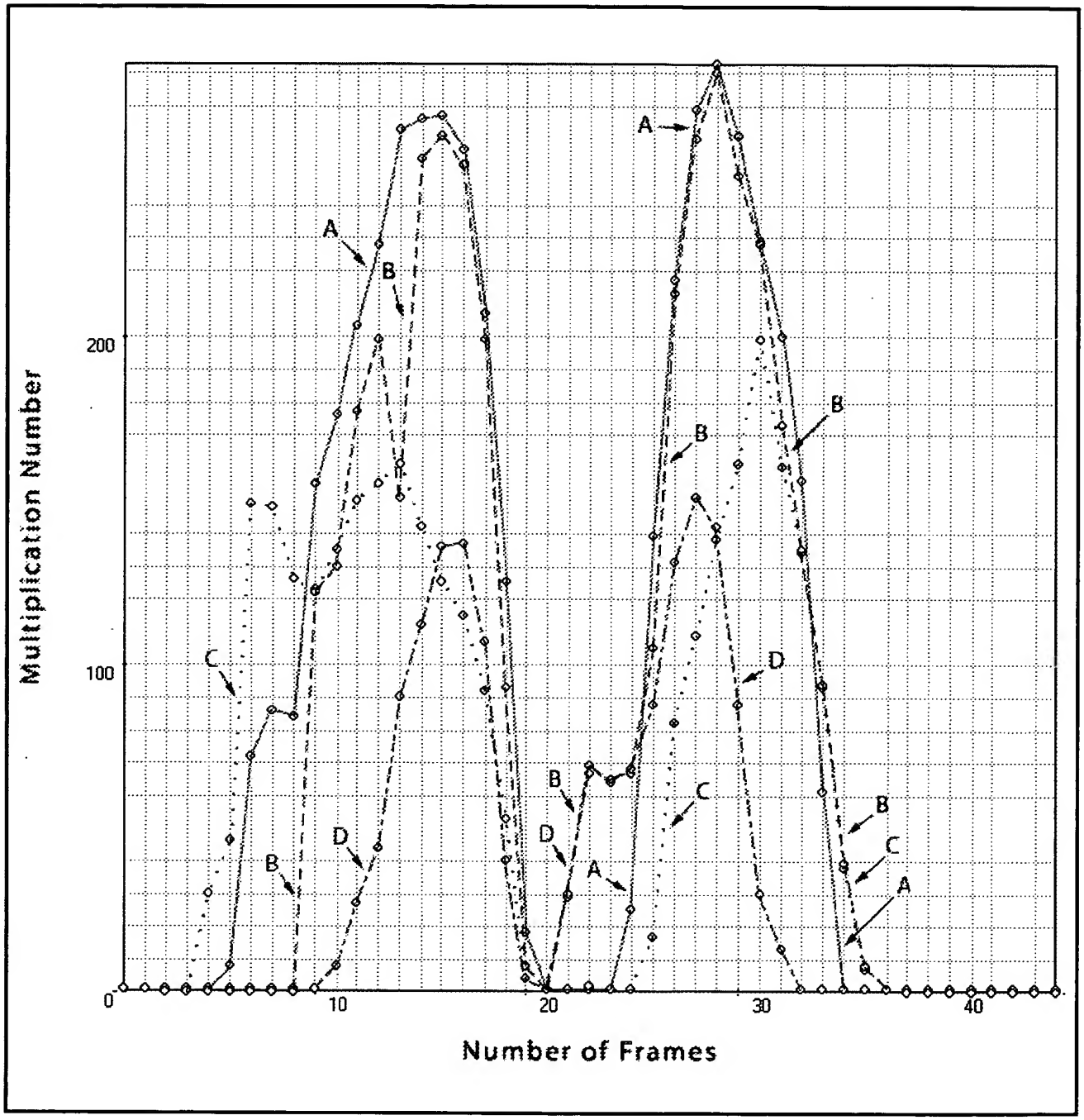

FIG. 28

Leonid Andreev, Dmitry Andreev. FIG. 29 of 43. A plot showing the multiplication number (M) changes in accordance with the walking motion frames shown in FIG. 27

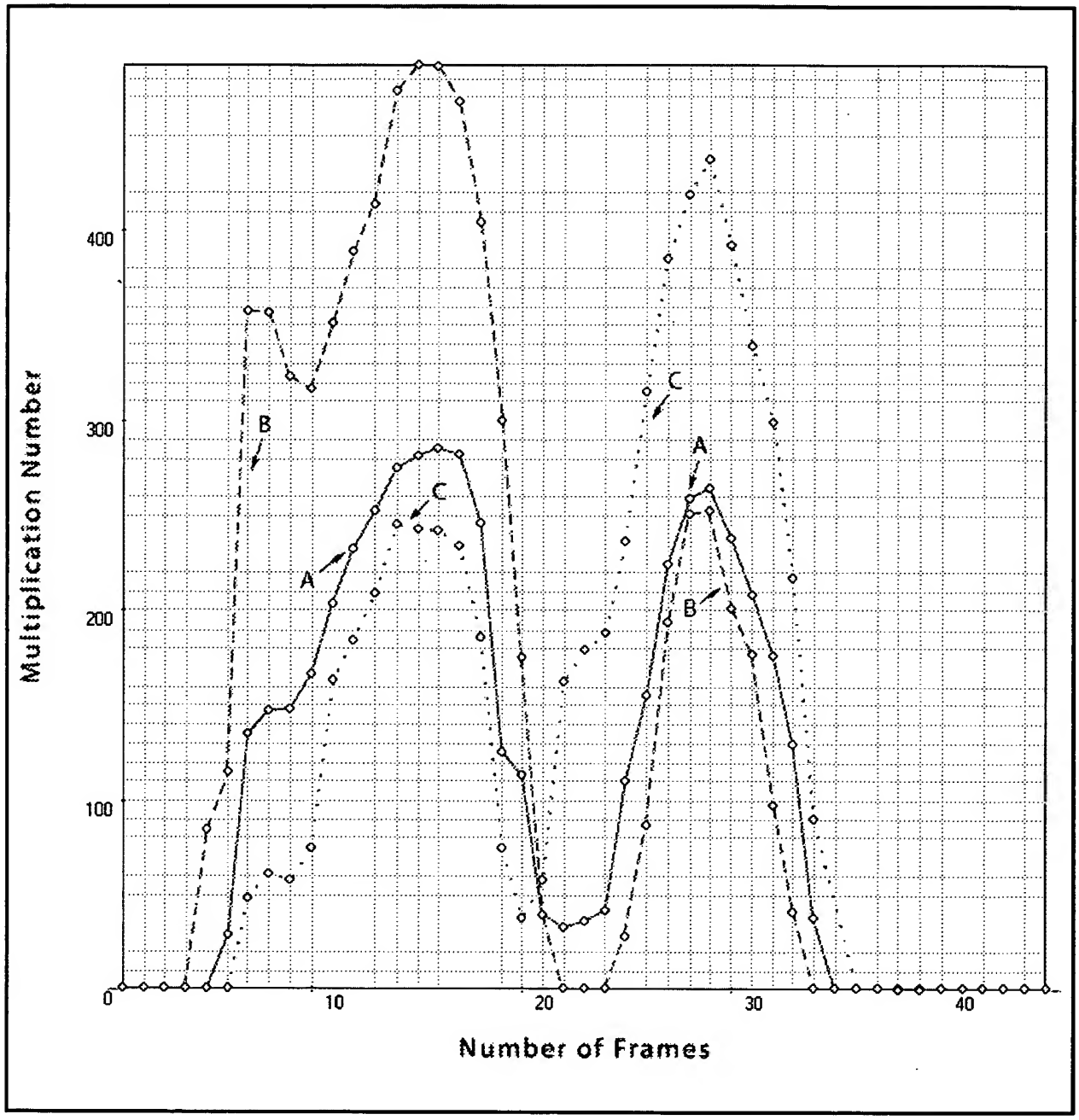

FIG. 29

Leonid Andreev, Dmitry Andreev. FIG. 30 of 43. A table for computation of a hybrid similarity matrix and identification of a target string in a sequence of *n*-elements

		Parameters				
		1	2	3	. . .	f
Objects	1	e_1	e_2	e_3	. . .	e_f
	2	e_2	e_3	e_4	. . .	e_{f+1}
	3	e_3	e_4	e_5	. . .	e_{f+2}
	.	.	.	.	. . .	.
	.	.	.	.	. . .	.
	k	e_k	e_{k+1}	e_{k+2}	. . .	e_{k+f-1}
	CC(k)	CC_k	CC_{k+1}	CC_{k+2}	. . .	CC_{k+f-1}
	.	.	.	.	. . .	.
	.	.	.	.	. . .	.
	k+f-1	e_{k+f-1}	e_{k+f}	e_{k+f+1}	. . .	e_{k+2f-2}
	.	.	.	.	. . .	.
	.	.	.	.	. . .	.
	n-f+1	e_{n-f+1}	e_{n-f+2}	e_{n-f+3}	. . .	e_n

FIG. 30

FIG. 31 of 43. Artificially generated signal pattern. Sections A and B are target objects for sequence recognition

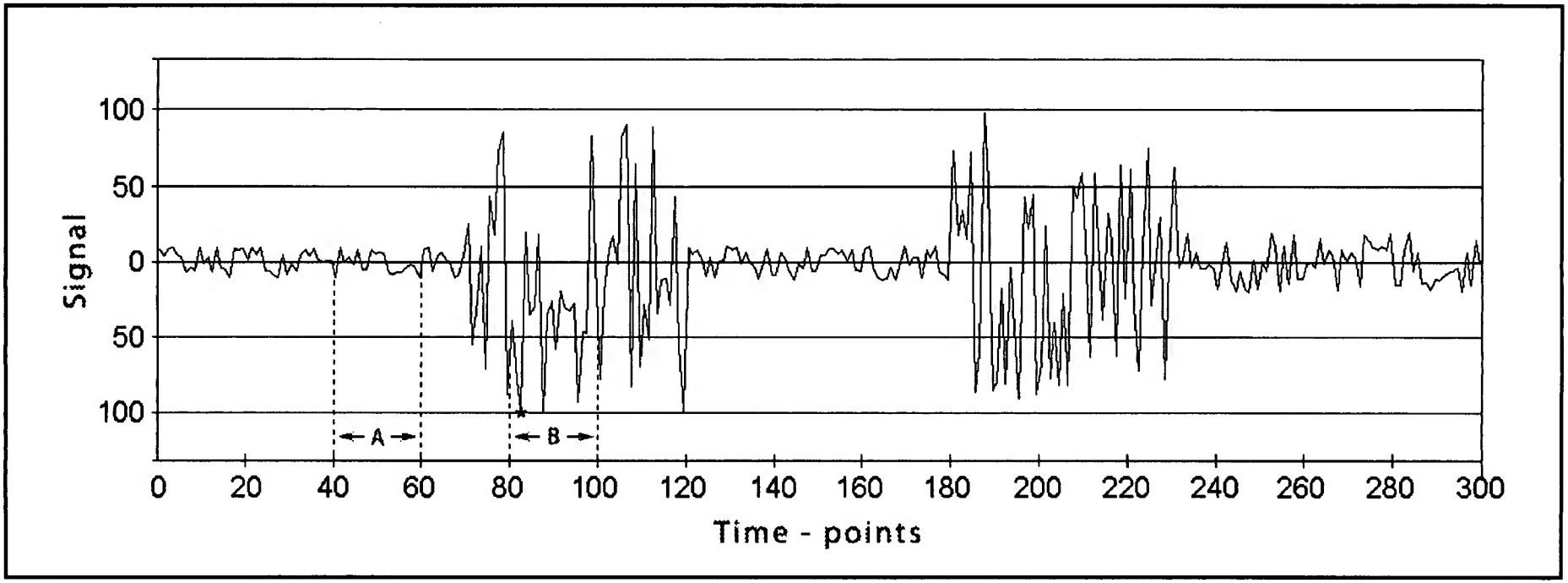

FIG. 31

Leonid Andreev, Dmitry Andreev.
FIG. 32 of 43. Result of sequence A (FIG. 31) recognition by method of this invention

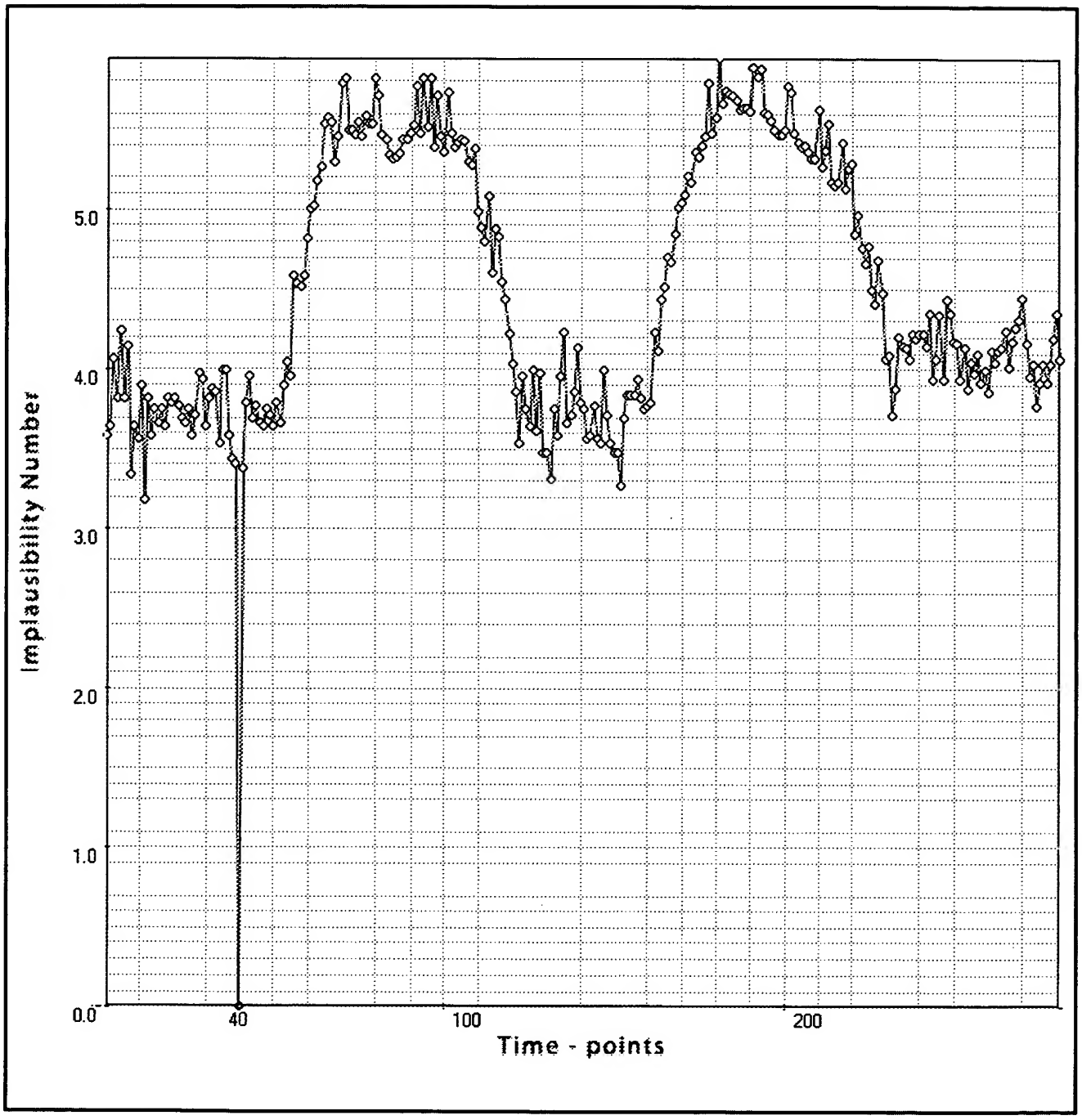

FIG. 32

Leonid Andreev, Dmitry Andreev.
FIG. 33 of 43. Result of sequence B (FIG. 31) recognition by method of this invention

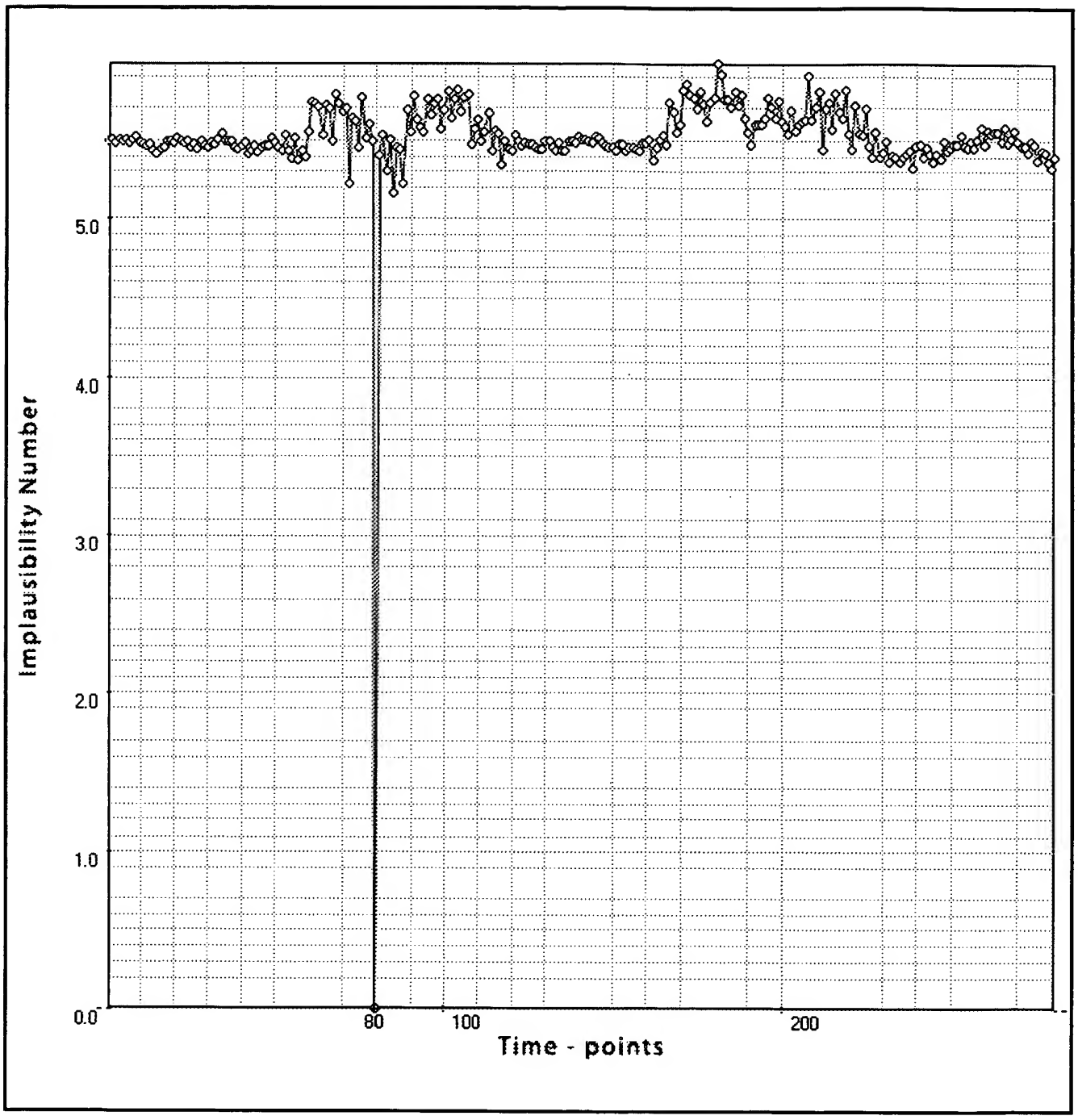

FIG. 33

Leonid Andreev, Dmitry Andreev.
FIG. 34 of 43. Relationship between the identification uncertainty computed for sequence B and the deviation from the value of the signal at time-point 83

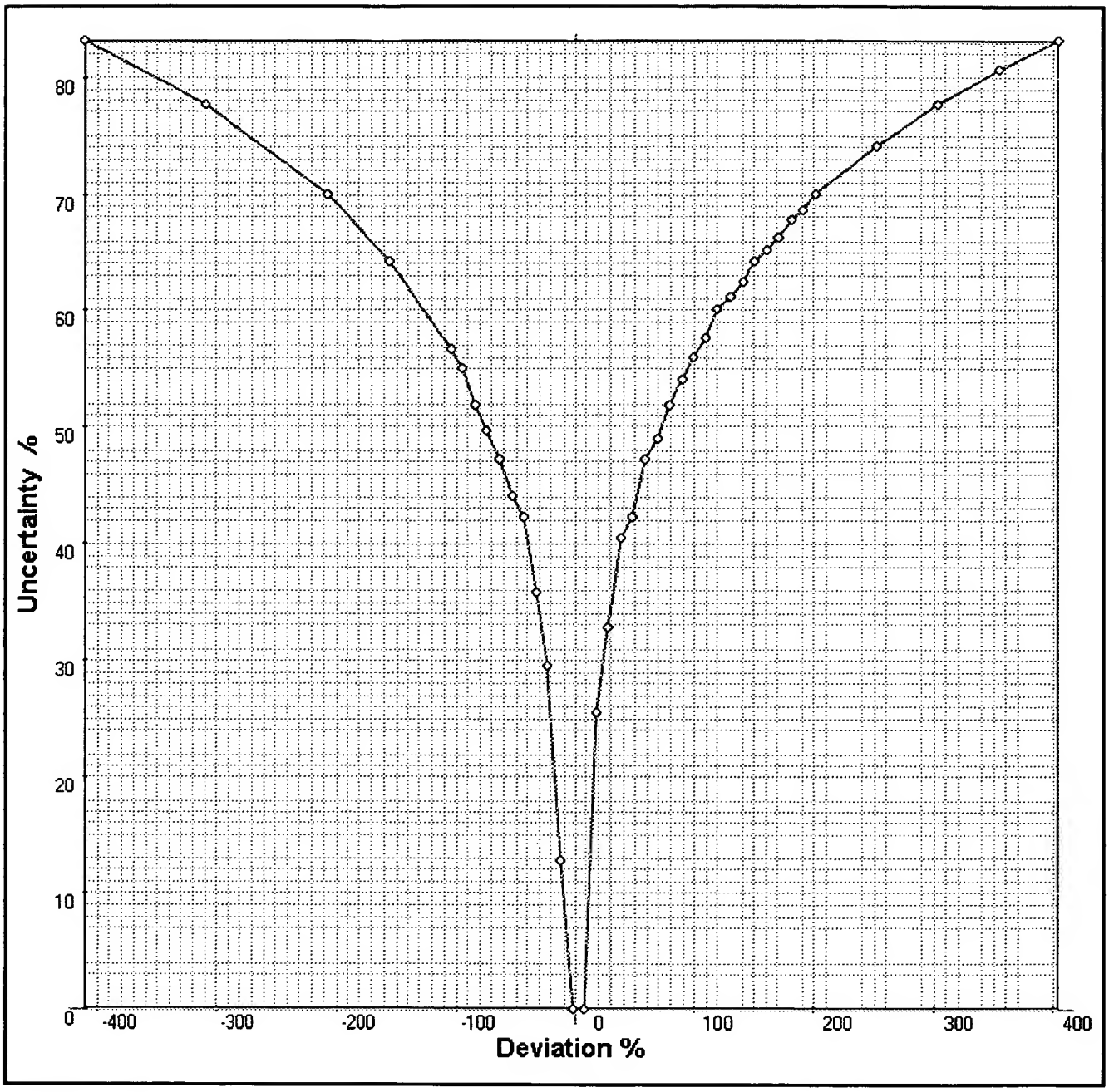

FIG. 34

Leonid Andreev, Dmitry Andreev.
FIG. 35 of 43. Artificially generated binary sequence. The section in bold is a reference string

1	2	3	4	5	6	7	8	9	10	11	12	13	14	15	16	17	18	19	20	
1	0	0	1	1	0	0	0	1	0	1	0	0	0	1	0	1	1	1	1	20
1	0	0	0	1	1	0	1	1	0	1	1	0	0	**1**	**1**	**1**	**1**	**1**	**1**	40
0	**0**	**1**	**0**	**1**	**0**	**1**	**0**	**1**	**1**	**0**	**1**	**0**	1	0	0	1	0	1	0	60
1	0	0	1	1	1	1	1	1	0	1	0	0	0	0	1	0	1	0	1	80
0	0	1	0	1	0	0	1	0	1	0	0	0	1	0	1	0	0	1	0	100
0	1	1	1	0	0	1	0	0	0	1	0	1	0	0	1	1	0	0	1	120
0	0	1	0	0	1	0	0	1	0	1	0	0	0	1	0	1	0	1	0	140
1	0	1	1	1	1	0	0	0	1	1	1	1	1	1	1	0	0	0	0	160
0	0	0	0	1	0	0	0	1	1	1	0	0	0	1	1	1	1	0	0	180

FIG. 35

Leonid Andreev and Dmitry Andreev.
FIG. 36 of 43. A table for computation of a similarity matrix used in binary sequence recognition

Object name	Value in HyPa	*M**	Parameters									
			31	32	33	34	35	36	37	38	39	40
Element 30	0.0	293	0.000	1.000	1.000	0.000	0.000	1.000	1.000	1.000	1.000	1.000
Element 31	0.0	243	1.000	1.000	0.000	0.000	1.000	1.000	1.000	1.000	1.000	1.000
Element 32	0.0	194	1.000	0.000	0.000	1.000	1.000	1.000	1.000	1.000	1.000	0.000
Element 33	0.0	244	0.000	0.000	1.000	1.000	1.000	1.000	1.000	1.000	0.000	0.000
Element 34	0.0	194	0.000	1.000	1.000	1.000	1.000	1.000	1.000	0.000	0.000	1.000
Element 35	0.0	1	1.000	1.000	1.000	1.000	1.000	1.000	0.000	0.000	1.000	0.000
Element 35, Clone 1	0.1	–	1.005	1.005	1.005	1.005	1.005	1.005	0.005	0.005	1.005	0.005
Element 35, Clone 2	0.2	–	1.010	1.010	1.010	1.010	1.010	1.010	0.010	0.010	1.010	0.010
Element 35, Clone 3	0.2	–	1.015	1.015	1.015	1.015	1.015	1.015	0.015	0.015	1.015	0.015
Element 35, Clone 4	0.3	–	1.020	1.020	1.020	1.020	1.020	1.020	0.020	0.020	1.020	0.020
Element 35, Clone 5	0.3	–	1.025	1.025	1.025	1.025	1.025	1.025	0.025	0.025	1.025	0.025
Element 35, Clone 6	0.4	–	1.030	1.030	1.030	1.030	1.030	1.030	0.030	0.030	1.030	0.030
Element 35, Clone 7	0.8	–	1.035	1.035	1.035	1.035	1.035	1.035	0.035	0.035	1.035	0.035
Element 35, Clone 8	0.8	–	1.040	1.040	1.040	1.040	1.040	1.040	0.040	0.040	1.040	0.040
Element 35, Clone 9	1.0	–	1.045	1.045	1.045	1.045	1.045	1.045	0.045	0.045	1.045	0.045
Element 35,Clone10	1.0	–	1.050	1.050	1.050	1.050	1.050	1.050	0.050	0.050	1.050	0.050
Element 36	0.0	194	1.000	1.000	1.000	1.000	1.000	0.000	0.000	1.000	0.000	1.000
Element 37	0.0	146	1.000	1.000	1.000	1.000	0.000	0.000	1.000	0.000	1.000	0.000
Element 38	0.0	244	1.000	1.000	1.000	0.000	0.000	1.000	0.000	1.000	0.000	1.000

* Multiplication Number

FIG. 36

Leonid Andreev, Dmitry Andreev. FIG. 37 of 43. A plot showing the changes in multiplication numbers as the screening frame in the form of the binary string (see FIG. 36) is moving along the binary sequence shown in FIG. 35.

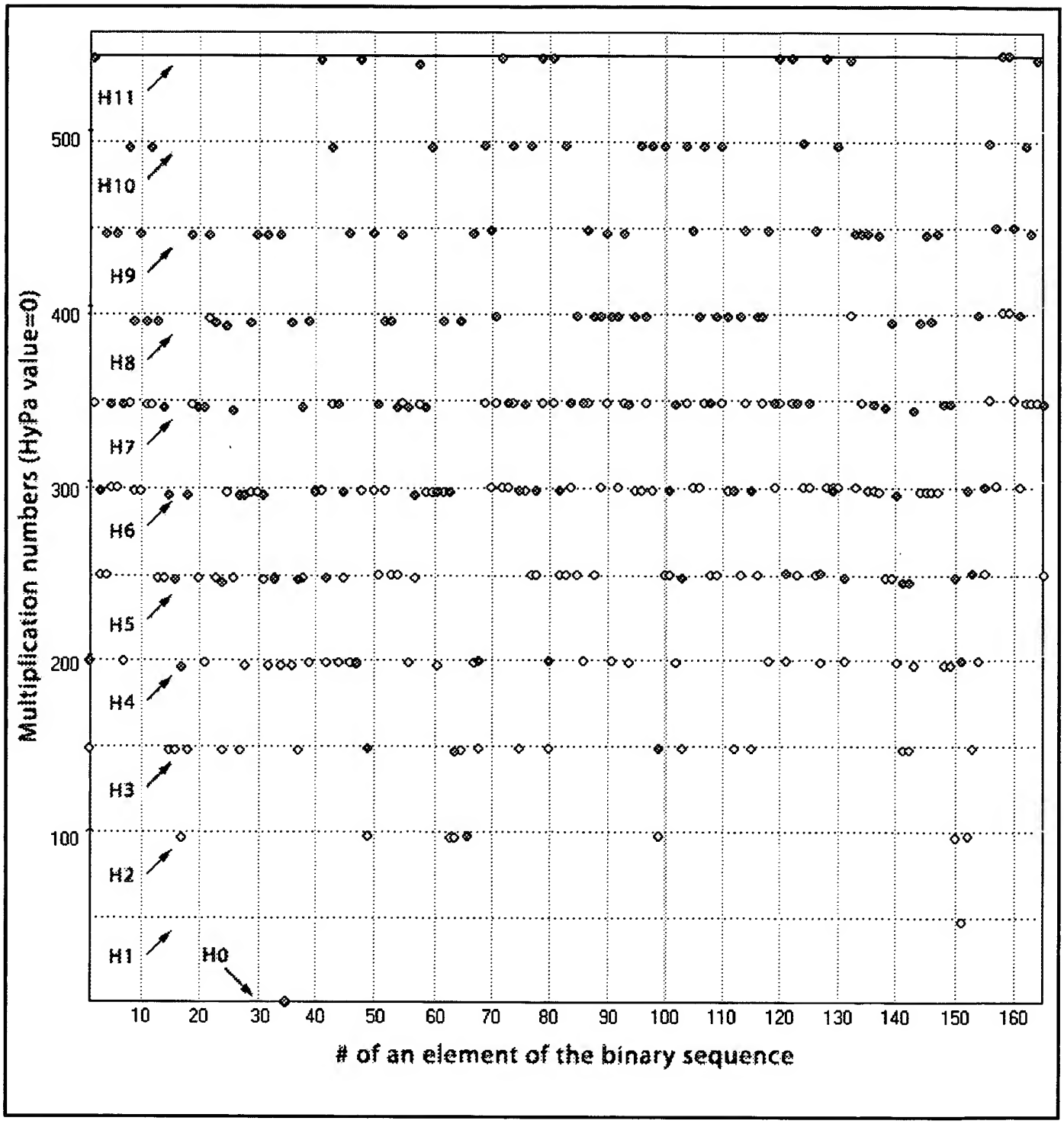

FIG. 37

Leonid Andreev, Dmitry Andreev. FIGS. 38A – 38B of 43. Correlation between implausibility numbers and demographic parameters of 220 countries under analysis

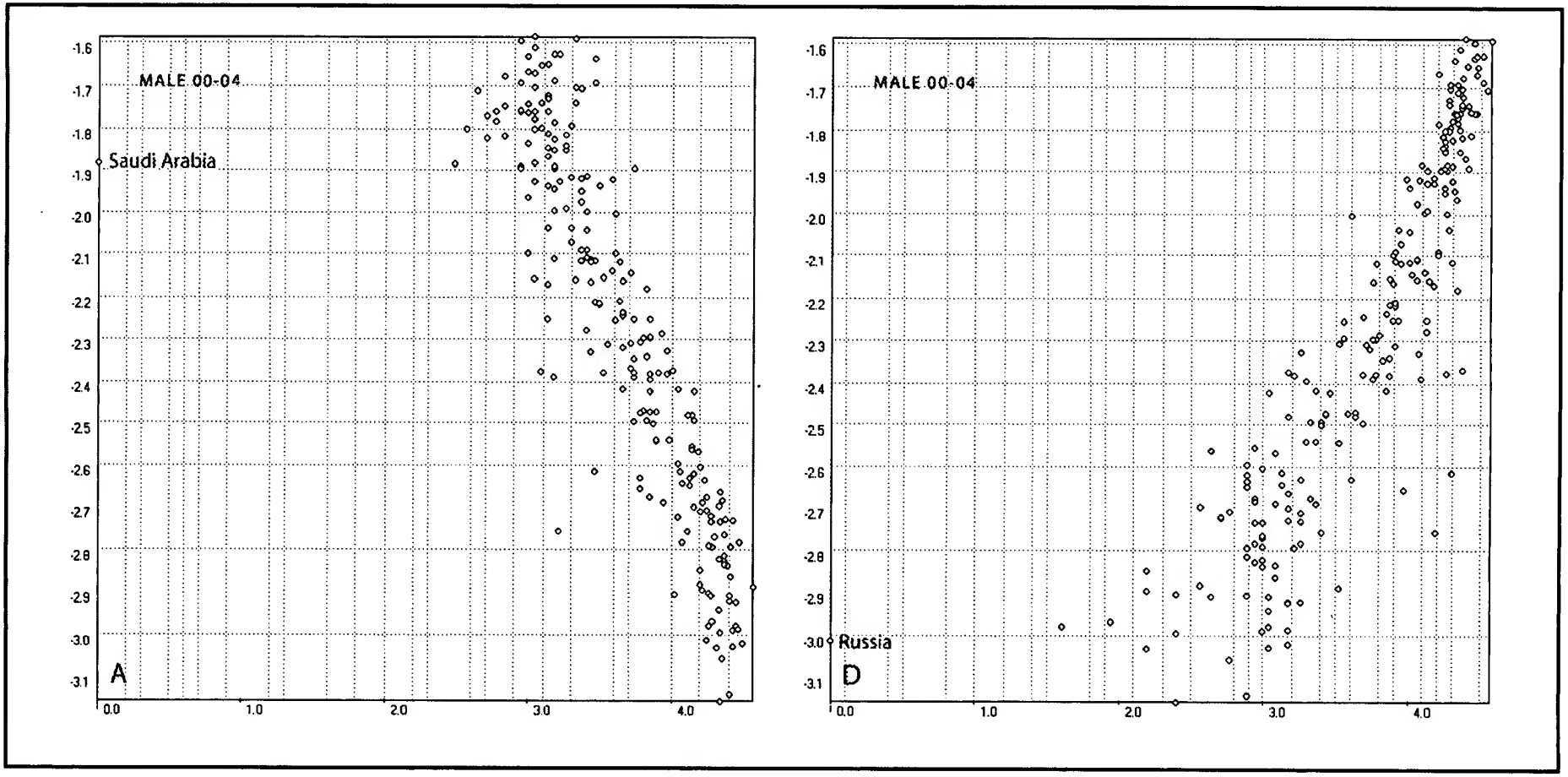

FIGS. 38A – 38B

Leonid Andreev, Dmitry Andreev. FIGS. 38C – 38D of 43. Correlation between implausibility numbers and demographic parameters of 220 countries under analysis.

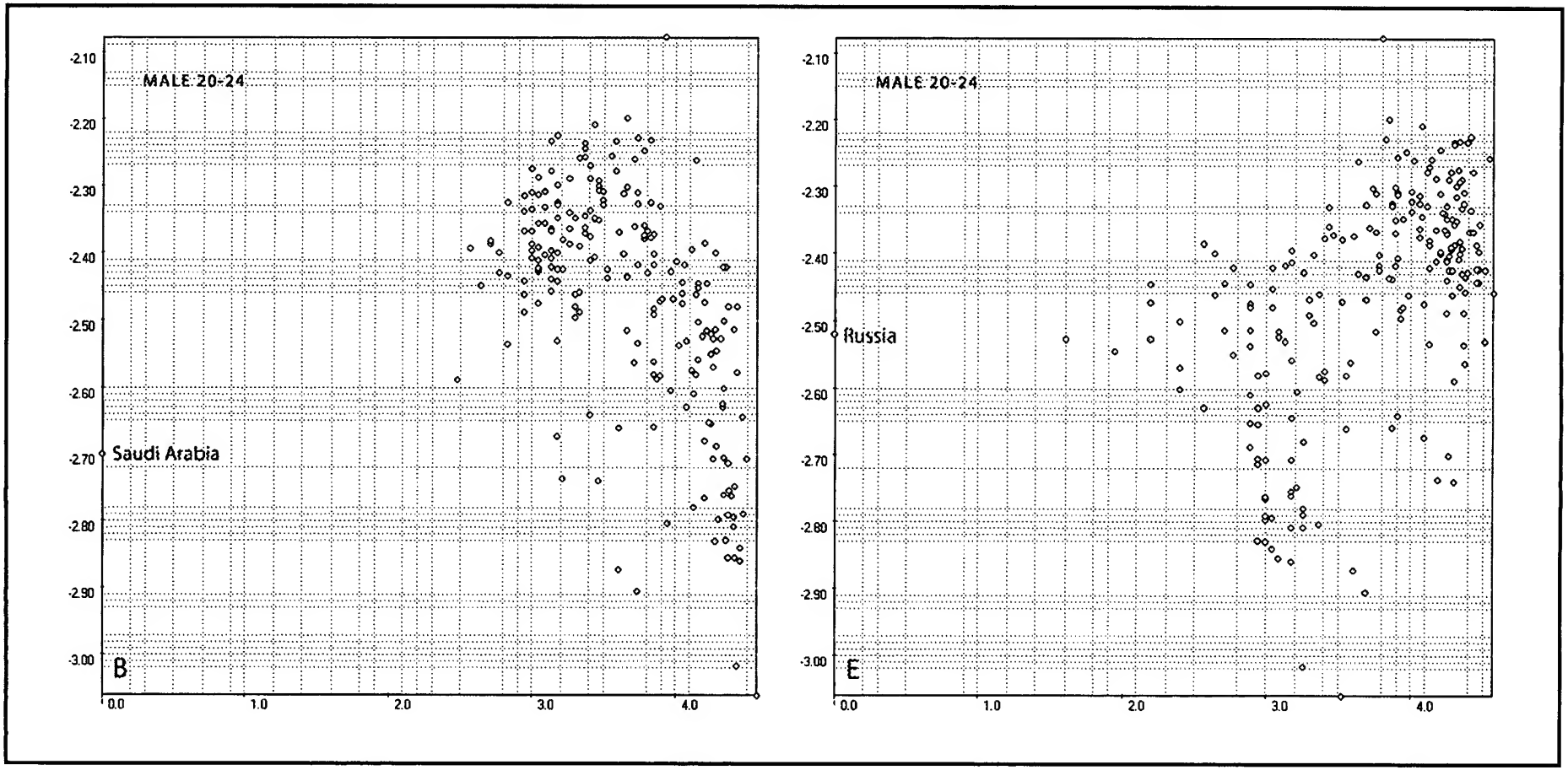

FIGS. 38C – 38D

Leonid Andreev, Dmitry Andreev. FIGS. 38E – 38F of 43. Correlation between implausibility numbers and demographic parameters of 220 countries under analysis.

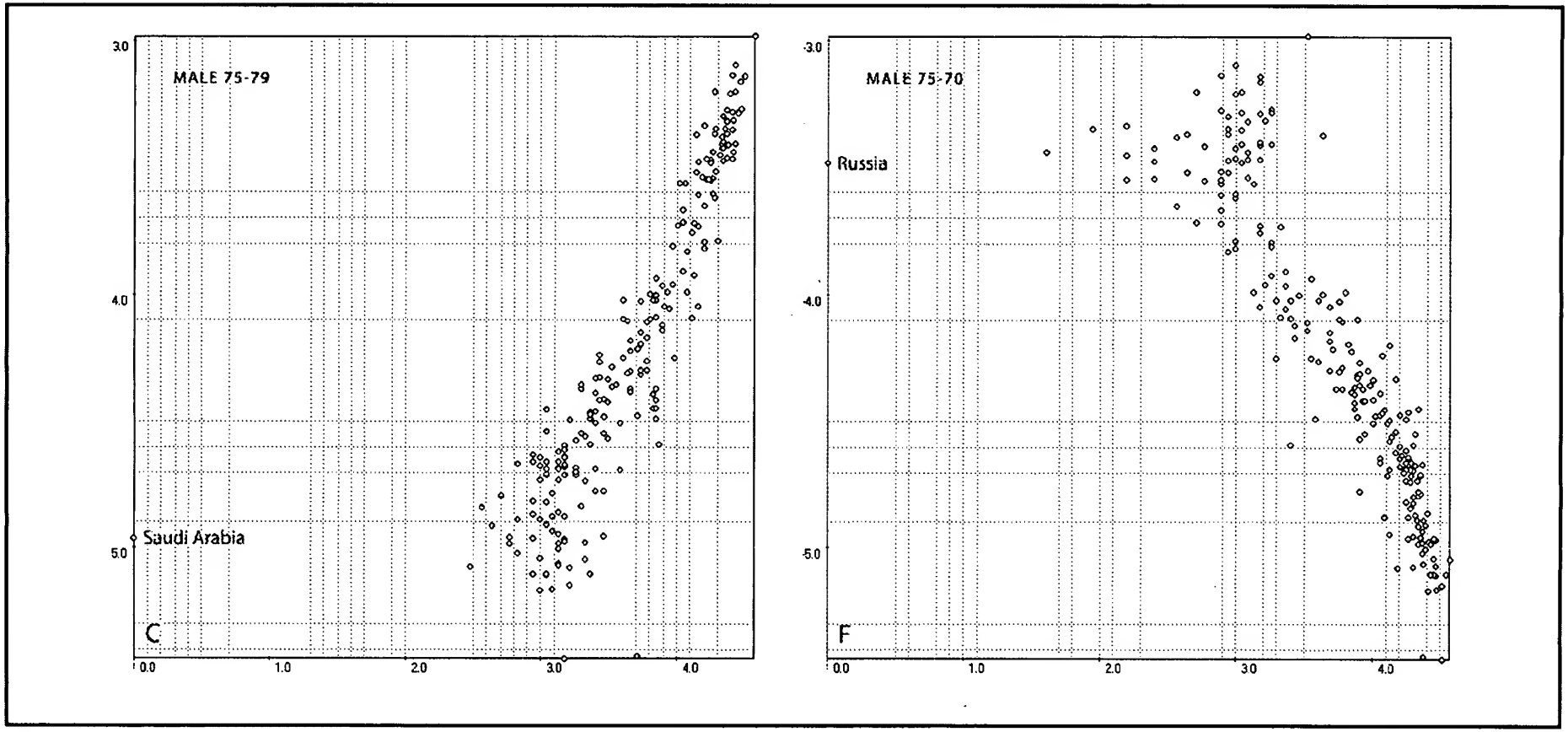

FIGS. 38E – 38F

Leonid Andreev, Dmitry Andreev. FIG. 39 of 43. Climatic data analysis by the HyGV-method. Relationship between values of February normal daily maximum temperatures (F°) and multiplication numbers computed for 245 cities and locations of 50 states the U.S.A., with Charleston, SC, as a reference object.

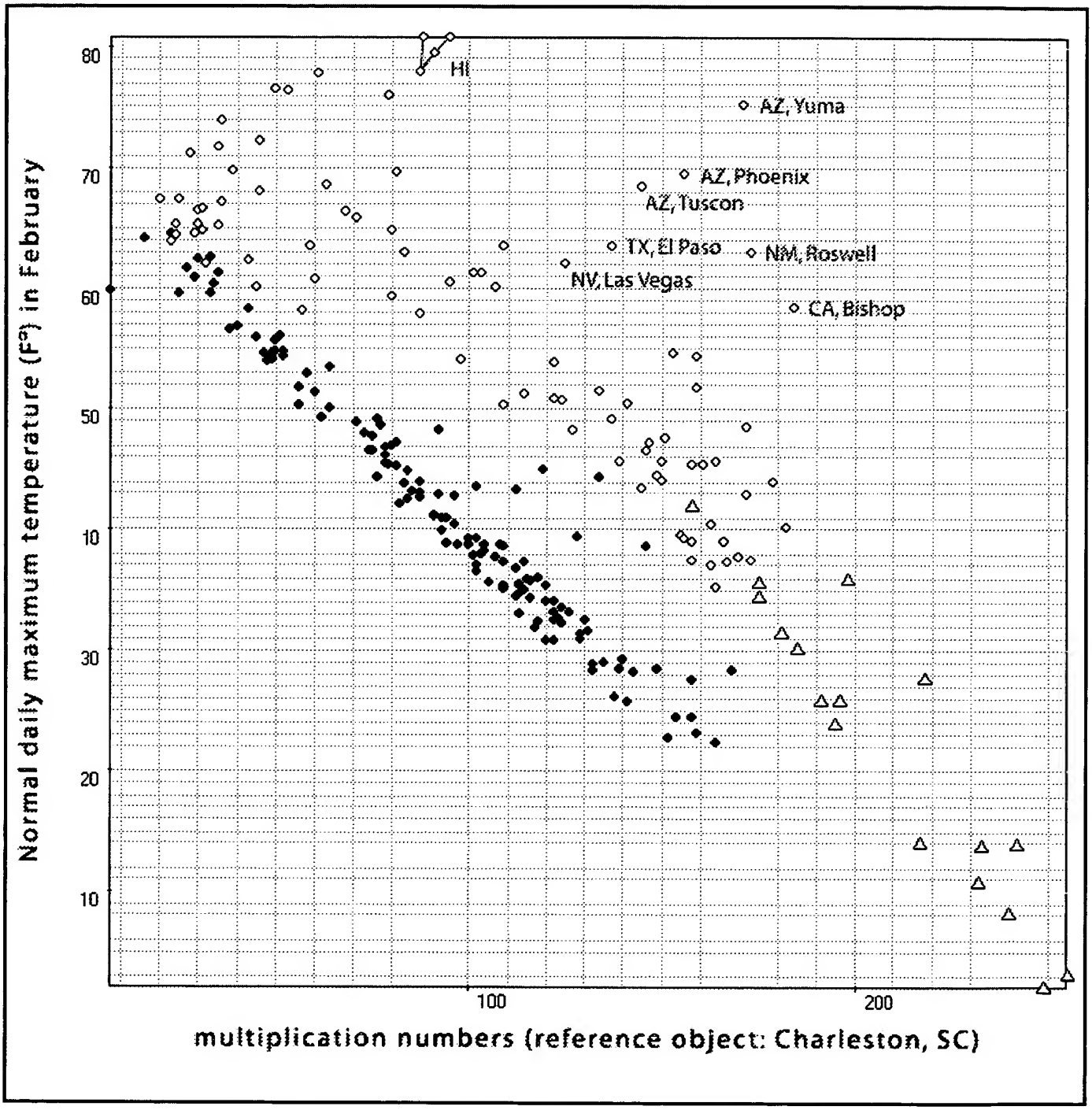

FIG. 39

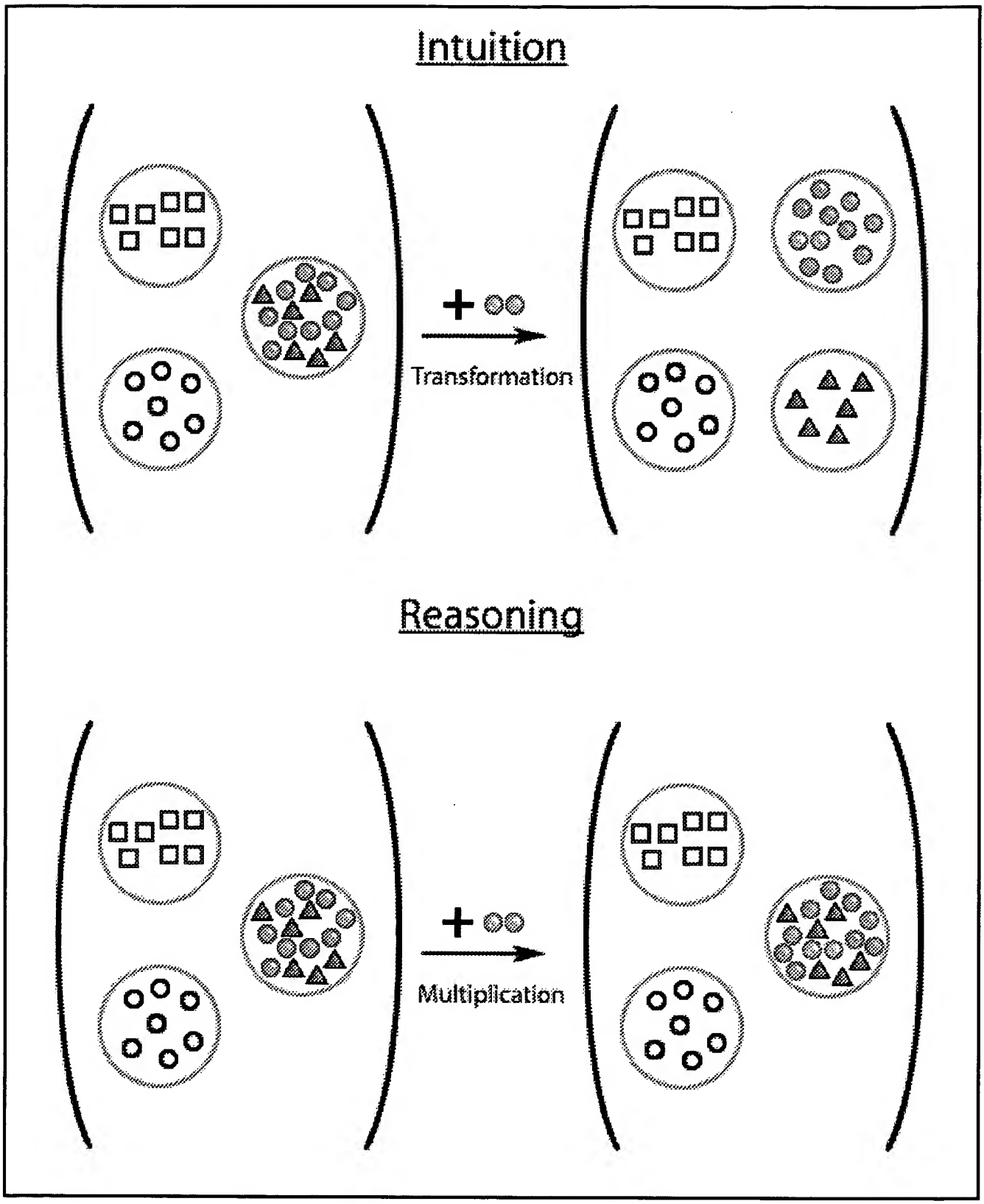

FIG. 40

Leonid Andreev, Dmitry Andreev. FIG. 41 of 43. Cluster trees showing the changes in the way of clustering that occur upon the addition of 1's to a natural sequence of numbers from 1 to 24.

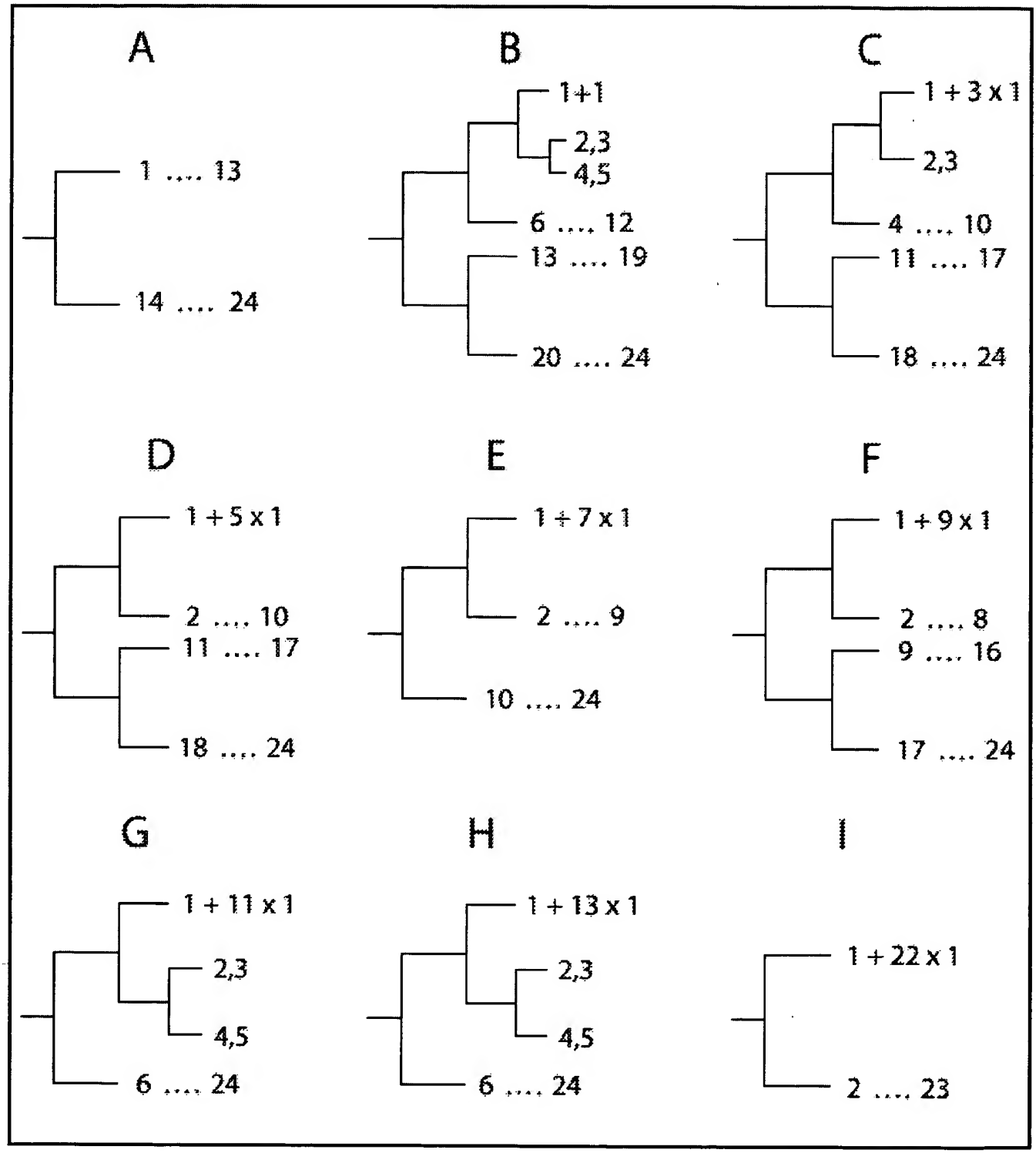

FIG. 41

Leonid Andreev, Dmitry Andreev. FIG. 42A of 43. HyPa self-evolution induced by consecutive addition of duplicates of analyzed objects to the capsule of clones

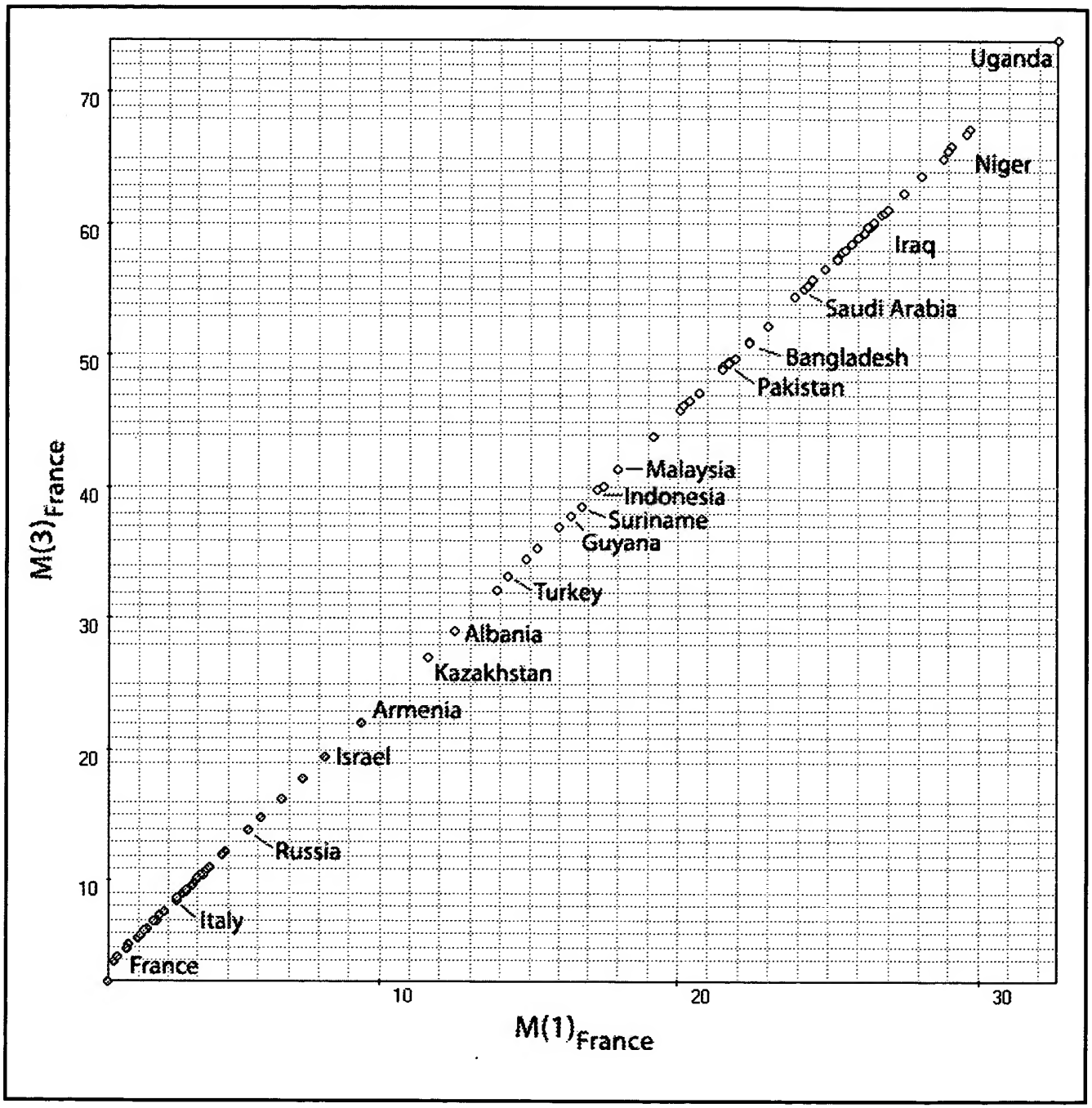

FIG. 42A

Leonid Andreev, Dmitry Andreev. FIG. 42B of 43. HyPa self-evolution induced by consecutive addition of duplicates of analyzed objects to the capsule of clones

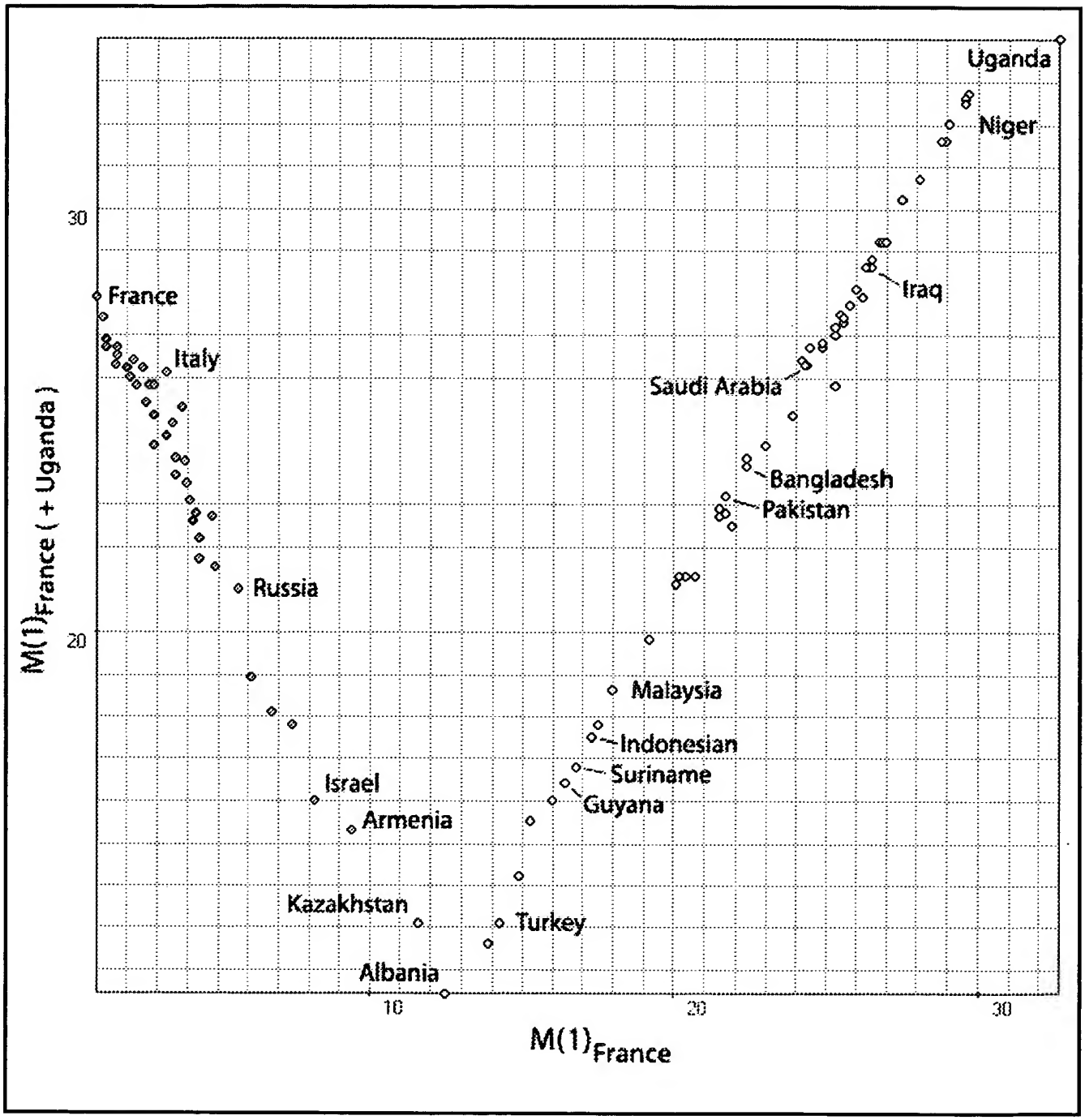

FIG. 42B

Leonid Andreev, Dmitry Andreev. FIG. 42C of 43. HyPa self-evolution induced by consecutive addition of duplicates of analyzed objects to the capsule of clones

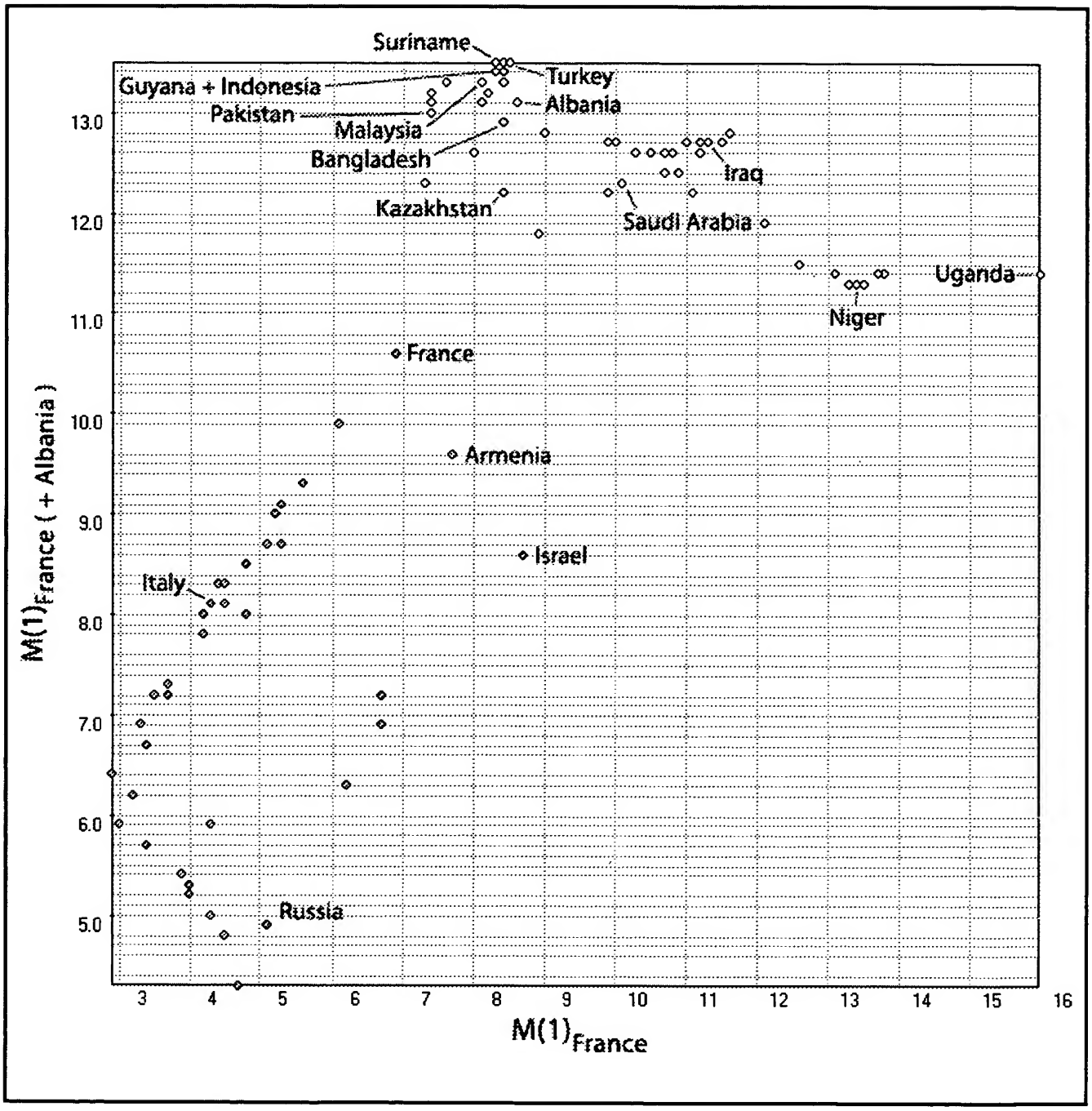

FIG. 42C

Leonid Andreev, Dmitry Andreev. FIG. 42D of 43. HyPa self-evolution induced by consecutive addition of duplicates of analyzed objects to the capsule of clones

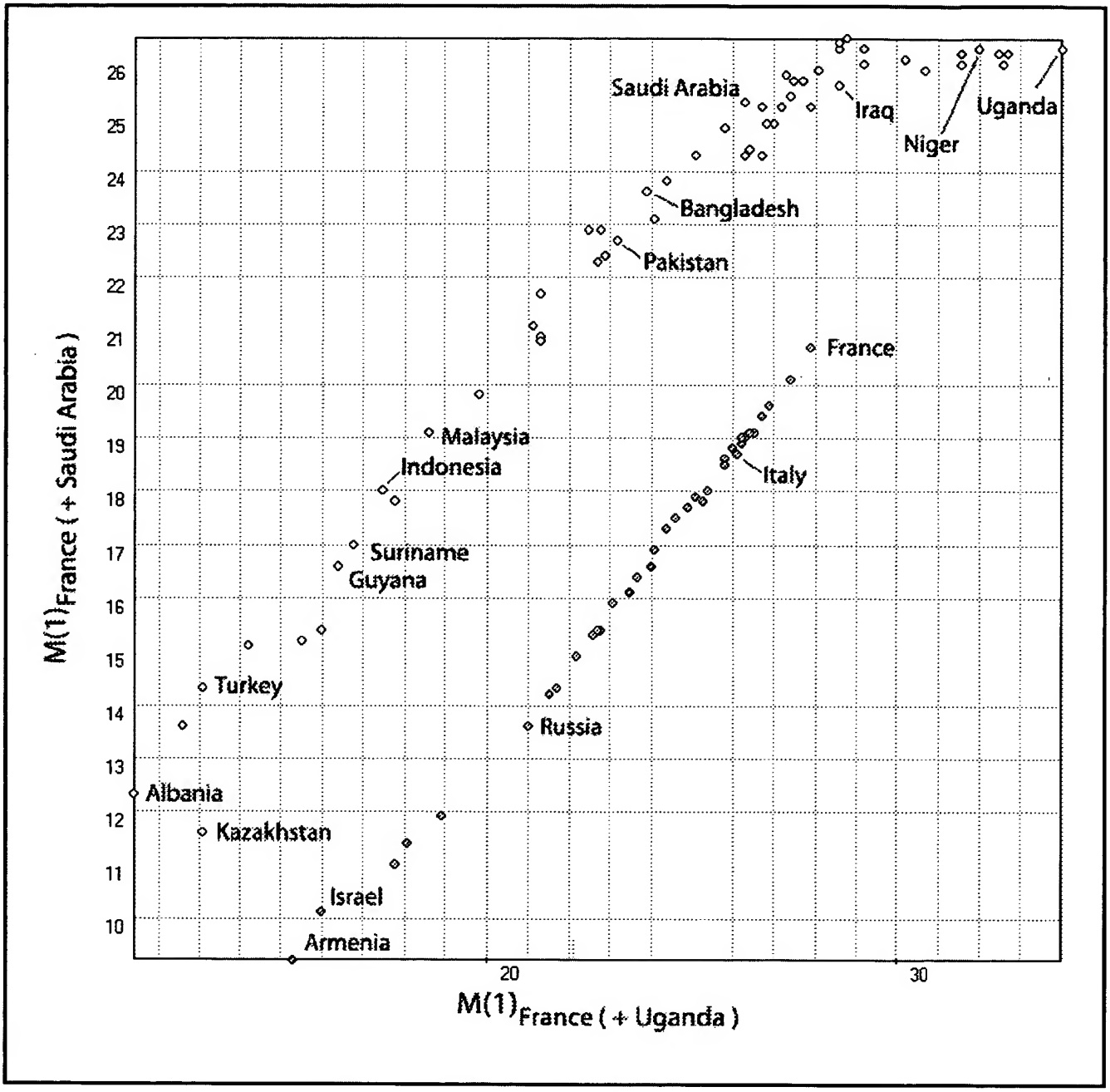

FIG. 42D

Leonid Andreev, Dmitry Andreev. FIG. 42E of 43. HyPa self-evolution induced by consecutive addition of duplicates of analyzed objects to the capsule of clones

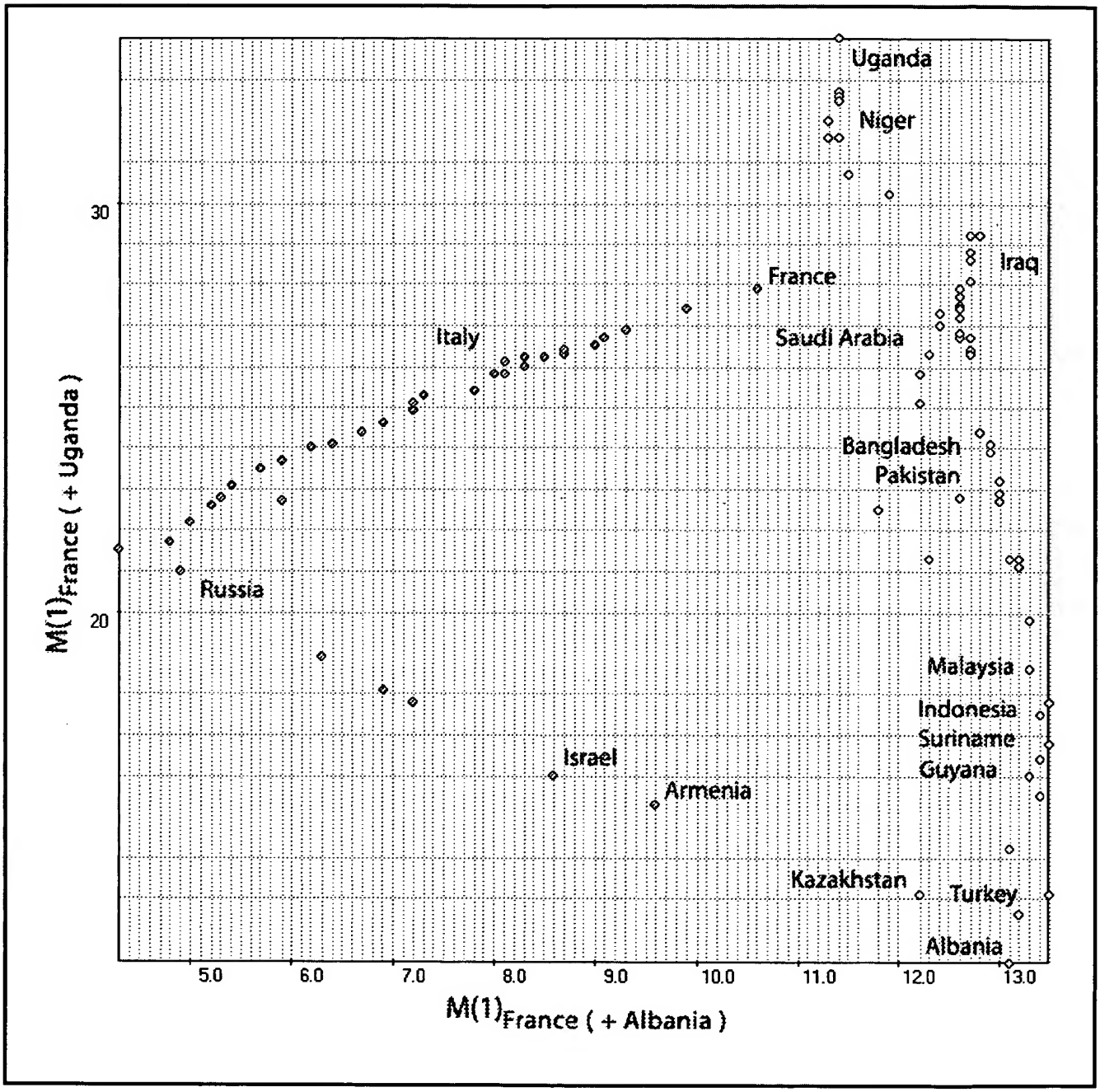

FIG. 42E

Leonid Andreev, Dmitry Andreev. FIG. 42F of 43. HyPa self-evolution induced by consecutive addition of duplicates of analyzed objects to the capsule of clones

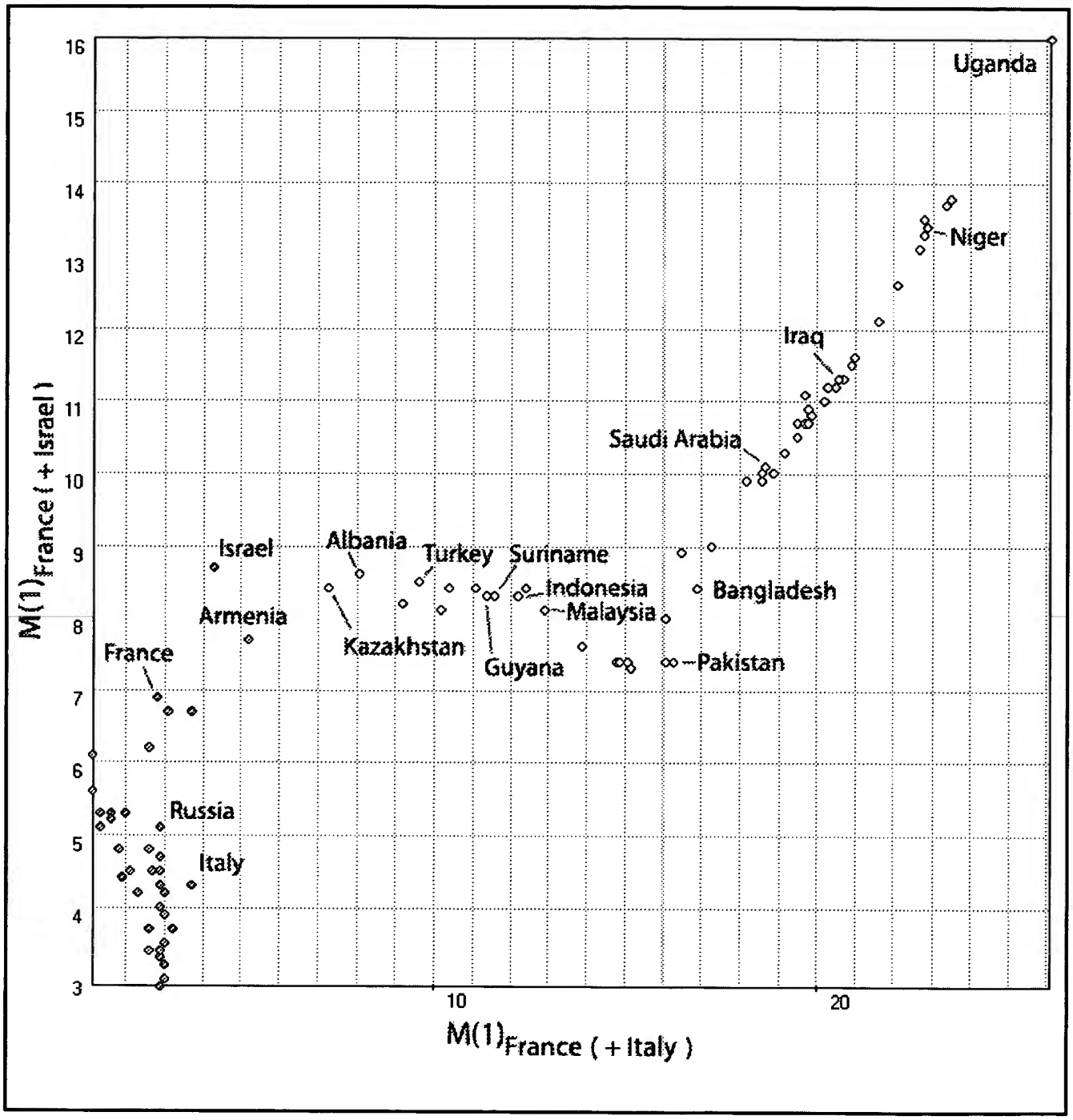

FIG. 42F

Leonid Andreev, Dmitry Andreev. FIG. 43 of 43. Search for image analogs by emphasizing certain parameters and shows the locations of analogs of the query pose (see FIG. 21) after the "R-Toe" parameter was emphasized by a 10-fold increase

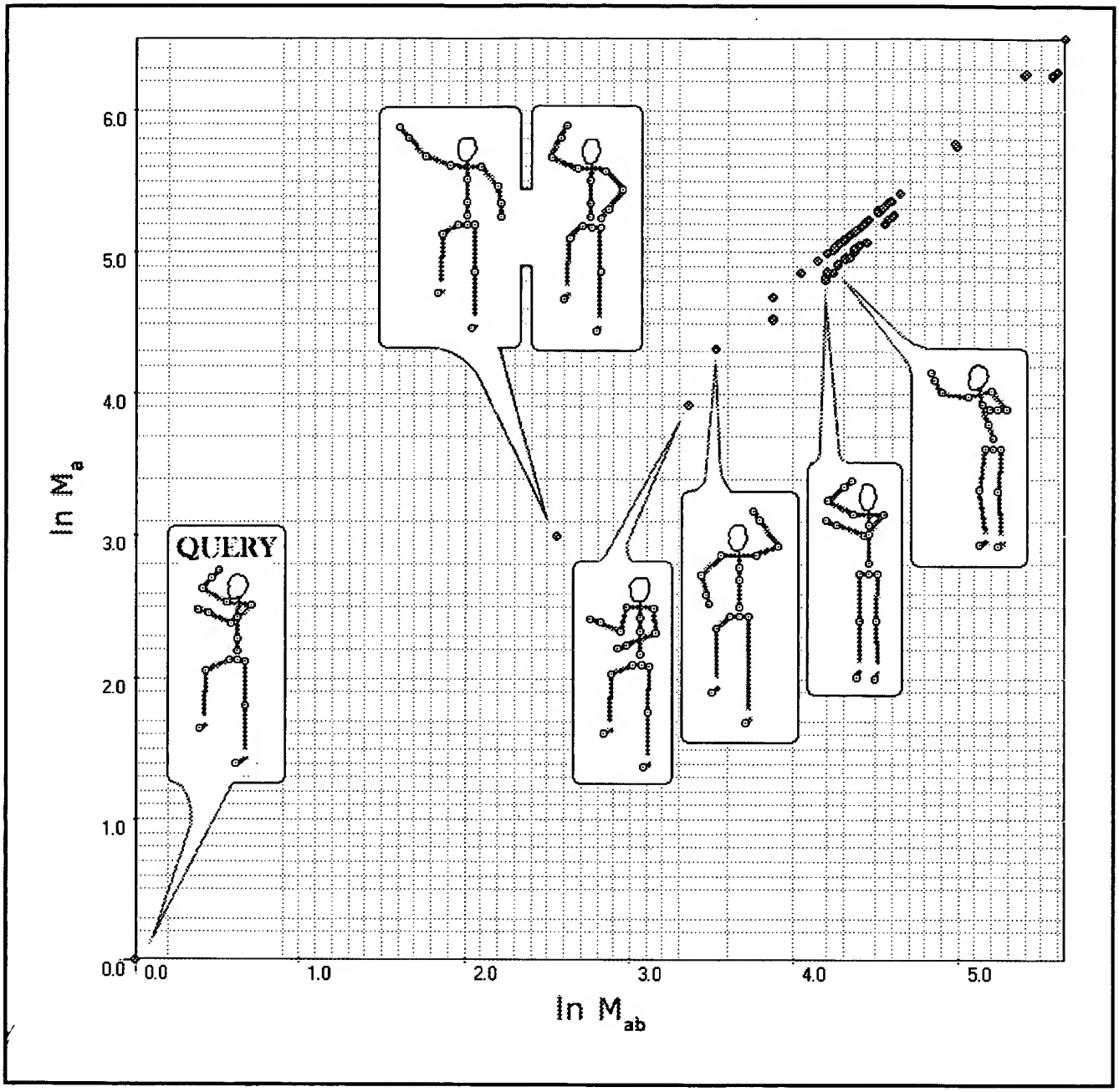

FIG. 43